CONTRACT REPORT ARBRL-CR-00393

HEAT TRANSFER STUDIES IN GUN TUBES

Prepared by

Science Applications, Inc.
8400 Westpark Drive
McLean, Virginia 22101

March 1979

US ARMY ARMAMENT RESEARCH AND DEVELOPMENT COMMAND
BALLISTIC RESEARCH LABORATORY
ABERDEEN PROVING GROUND, MARYLAND

Destroy this report when it is no longer needed.
Do not return it to the originator.

Secondary distribution of this report by originating or sponsoring activity is prohibited.

Additional copies of this report may be obtained from the National Technical Information Service, U.S. Department of Commerce, Springfield, Virginia 22161.

The findings in this report are not to be construed as an official Department of the Army position, unless so designated by other authorized documents.

The use of trade names or manufacturers' names in this report does not constitute indorsement of any commercial product.

REPORT DOCUMENTATION PAGE		READ INSTRUCTIONS BEFORE COMPLETING FORM
1. REPORT NUMBER CONTRACT REPORT ARBRL-CR-00393	2. GOVT ACCESSION NO.	3. RECIPIENT'S CATALOG NUMBER
4. TITLE *(and Subtitle)* HEAT TRANSFER STUDIES IN GUN TUBES		5. TYPE OF REPORT & PERIOD COVERED Final Report 6. PERFORMING ORG. REPORT NUMBER SAI-78-719-WA
7. AUTHOR(s) P. L. Versteegen F. D. Varcolik		8. CONTRACT OR GRANT NUMBER(s) DAAK-77-C-0052
9. PERFORMING ORGANIZATION NAME AND ADDRESS Science Applications, Inc. 8400 Westpark Drive McLean, Virginia 22101		10. PROGRAM ELEMENT, PROJECT, TASK AREA & WORK UNIT NUMBERS
11. CONTROLLING OFFICE NAME AND ADDRESS US Army Armament Research & Development Command US Army Ballistic Research Laboratory (DRDAR-BL) Aberdeen Proving Ground, MD 21005		12. REPORT DATE March 1979 13. NUMBER OF PAGES 64
14. MONITORING AGENCY NAME & ADDRESS(*if different from Controlling Office*)		15. SECURITY CLASS. (*of this report*) UNCLASSIFIED 15a. DECLASSIFICATION/DOWNGRADING SCHEDULE

16. DISTRIBUTION STATEMENT *(of this Report)*

Approved for public release; distribution unlimited.

17. DISTRIBUTION STATEMENT *(of the abstract entered in Block 20, if different from Report)*

18. SUPPLEMENTARY NOTES

19. KEY WORDS *(Continue on reverse side if necessary and identify by block number)*

Heat Transfer
Conduction
Gun Tubes
Temperature
Rotating Band
Coatings

20. ABSTRACT *(Continue on reverse side if necessary and identify by block number)*

A number of heat transfer studies have been performed in gun tube geometries especially those using folded ammunition. These analyses included the evaluation of the peak surface temperature using a new set of boundary conditions, time-dependent heat transfer coefficients and bulk fluid temperatures. The effects of uncertainties in the thermal properties and the effect of three surface coating materials were evaluated. A three-dimensional model of part of the folded ammunition geometry was developed and temperature histories for it were calculated over four rounds of firing. A thermal model was developed

20. (cont'd)

describing the temperature histories of a block sliding over a stationary surface. This model is an attempt at evaluating the thermal conditions in a rotating band. The preliminary results are very encouraging.

TABLE OF CONTENTS

LIST OF FIGURES

LIST OF FIGURES (cont.)

LIST OF TABLES

Section 1

INTRODUCTION

The analyses and results described in this report are a continuation of a study to investigate heat transfer phenomena in folded ammunition gun tubes. The initial work by the authors was reported in Reference 1. This initial effort established the geometry, validated TRUMP, a generalized heat transfer computer program, for problems of interest, developed the methodology to implement the detailed boundary conditions that were provided by the Ballistic Research Laboratory, and generated results for certain geometries and conditions of interest. The present effort consists primarily of evaluating the effects of a new set of boundary conditions (2), that is, time-dependent heat transfer coefficients and bulk fluid temperatures, and sensitivities due to uncertainties in the thermal properties of the two materials that enter into the problem, namely, gun tube steel and cartridge brass. In addition, the effect on the peak surface temperature was evaluated for three coating materials, namely, chromium, tungsten, and molybdenum. Several aspects related to three-dimensional effects of the folded ammunition geometry were investigated, including multiple firing. Furthermore, the generalized heat transfer program used in all of these calculations was evaluated with respect to its suitability in determining temperature distributions in the presence of a moving boundary, such as the case of a rotating band.

Section 2

GEOMETRY, BOUNDARY CONDITIONS AND THERMAL PROPERTIES

The primary geometry of interest is the same as the one discussed in the previous study (1). Figure 1 is reproduced from there and shows with an asterisk (*) the region of the geometry where several analyses are given in this report. Other analyses are performed for the region near the origin of rifling. Figure 2, also taken from Reference 1, shows a cross-section of the folded ammunition gun tube chamber for which a three-dimensional analysis with multiple firing is performed. The time-dependent boundary conditions are given as a function of distance along the tube. The locations for which this information is given is shown in Figure 3. These distances are translated to the folded geometry by aligning them along the inside of the gun tube chamber, along either side of the web between the powder chamber and the projectile. The boundary conditions consisted of time-and space-dependent heat transfer coefficients, h, and bulk fluid temperatures, T_b. The heat flow per unit surface area, q", into the gun barrel was then defined as

$$q''(z,t) = h(z,t)\,[T_b(z,t) - T_s(z,t)]$$

where $T_s(z,t)$ is the gun barrel surface temperature to be determined, t is the elapsed time, and z is the distance along the gun barrel. Since the boundary conditions data set is too large to be presented here in total, only a few typical curves will be shown here. Figures 4 and 5 show time histories of heat transfer coefficients and bulk fluid temperatures at several typical locations. A comparison between the new (2) and old data (1) sets are shown in Figures 6 and 7. It may be noted that the present data set reflects a much cooler propellant and hence lower surface temperature can be expected.

For the peak surface temperature calculations with the new set of boundary conditions, the thermal properties of the materials are the same as those from the previous study. Table 1 repeats them for reference. This was done to ensure that proper comparisons can be made between the present and previous results.

For those calculations that involved sensitivity with respect to the uncertainty in the values of the thermal properties a literature search was made to determine the most up-to-date values and their range. This was also done for the plating materials that were studied. The thermal properties of all of these materials, thermal conductivity and specific heat, are shown in Figures 8 through 17. The materials considered in this study are:

- SAE 4340 steel (gun tube steel)
- 70/30 brass (cartridge brass)
- chromium
- tungsten
- molybdenum

The data points on these curves are various data sets extracted from the volumes published by Touloukian et al. (3, 4) and the critical review of Ho et al. (5). Since TRUMP accepts thermal property information in tabular form and interpolates linearly into these tables to evaluate their temperature dependence, it was found simplest to draw straight line segments through the experimentally determined properties. These straight line segments are shown in Figures 8 through 17. The values given at the breakpoints of these line segments are then used as input data to TRUMP. These are summarized in Table 1. For comparison purposes, the data used in the previous study are shown in Table 2.

Table 1. Thermal Properties of Various Materials for TRUMP.

Material	Temperature ^{o}C	Thermal Conductivity watt/cm-^{o}C	Temperature ^{o}C	Specific Heat J/g-^{o}C
SAE 4340	0	0.349	-23.	.046
	100	0.374	467.	.064
	200	0.382	677.	.092
	300	0.376	707.	.28
	400.	0.363	747.	.074
	500	0.347	777.	.064
	600	0.333	1200.	.064
Cartridge Brass	-53.	0.95	-23.	0.42
	212.	1.415	182.	0.42
	337.	1.490	234.	0.50
	427.	1.462	267.	0.45
			927.	0.45
Chromium	-23.	1.0	-73.	0.40
	27.	0.935	132.	0.49
	97.	0.925	592.	0.55
	577.	0.687	927.	0.70
	927.	0.620		
Tungsten	-73.	1.87	0.	0.134
	222.	1.46	1000.	0.155
	327.	1.37		
	427.	1.30		
	627.	1.21		
	927.	1.13		
Molybdenum	0.	1.39	0.	0.256
	500.	1.21	550.	0.281
	1000.	1.03	1000.	0.310

Table 2. Thermal Properties of Materials

Material \ Properties	Specific Heat (J/kg-C)	Temperature (C)	Thermal Conductivity (W/m-C)	Temperature (C)
	502.	-18.05	43.1	-18.05
	519.	204.	42.3	204.
	619.	427.	38.6	427.
SAE 4340	753.	648.	32.2	648.
Density: 7,750 kg/m^3	800.	763.	25.9	788.
Melting Point: 1450^{o}C	6895.*	768.	27.0	871.
	628.	773.		
	586.	871.		
	607.	1094.		
	398.	0.	96.	0.
Cartridge Brass	490.	200.	105.	100.
Density: 8,570 kg/m^3	527.	500.	109.	200.
Melting Point: 940^{o}C			113.	300.
			115.	400.

*SAE 4340 steel has a solid phase change at $\sim$ 768^{o}C. The latent heat involved in this transition is modeled by a change in specific heat in the form of a spike superimposed over the actual specific heat curve. This triangular peak has a base width of 10^{o}C, a height of 1/5 of the latent heat of transition and is centered at the transition temperature.

Section 3

ANALYSIS TECHNIQUES

3.0 GENERAL ASPECTS

All analyses performed in this report were made with the TRUMP heat transfer computer program (6). A brief description of the general capabilities of this code were given in the previous study (1) and will not be repeated here. TRUMP has been used successfully at SAI over the past several years on a multitude of heat transfer problems. Because the code was developed to solve problems with complex geometries the preparation of input data to TRUMP is a time consuming process, especially when parameter studies are to be made that involve a redefinition of the geometry and node structure. Experience has shown that such problems are most easily handled by developing an input data generator for the geometry and boundary conditions under investigation. The node generator computes all the BLOCK4 and BLOCK5 data required by TRUMP and stores these on a file which is later read and processed by the TRUMP program. The BLOCK4 data consists of the node characteristic descriptions, that is, their number, volume, and material type. The BLOCK5 data contains all information about how the various nodes are connected, that is, conduction lengths, heat transfer surface area, convection heat transfer coefficients, and thermal radiation form factors. These two blocks contain the bulk of the data preparation chores.

For the present studies several node generators were written, each applicable to a specific geometry and sets of boundary conditions. These are discussed briefly in the next several sections. In addition to these node generators a number of modifications were made to TRUMP in the form of additional FORTRAN statements and subroutines. These modifications were necessary to handle the different problem requirements. The various programs and special TRUMP subroutines are listed below with a brief comment.

TCY1 - a node generator that computes the data for one-dimensional rectangular and cylindrical problems.

TODXY - a node generator that computes the data for a two-dimensional rectangle which may have a radius on one corner.

THREED - a node generator that computes the data for a three-dimensional slice of the cross section C-C shown in Figures 1 and 2.

ROTBAND - a node generator to compute the data for the rotating band problem discussed in more detail in Section 3.4.

HTCOF0, HTCOF1, HTCOF2 - Subroutines for TRUMP to process the boundary conditions as needed.

DINAM - a TRUMP subroutine to modify and keep track of the dynamic connections when running the rotating band problem.

HTSORT - a program to prepare the boundary conditions in a form suitable for processing by TRUMP.

DIMENS - a program to set FORTRAN dimension statements and common blocks to sizes specified on the input data. Used on TRUMP to create a version with a large number of nodes and connections required for the three-dimensional problems.

TMPPOST - a post-processor program that reads the results file created by TRUMP and displays selected results.

TUBE - a driver program for the GRAPH routine package that produces printer plots of the boundary conditions, i.e., heat transfer coefficients and bulk fluid temperatures as a function of time for each of the axial locations.

DETAIL - a program that prints the detailed results produced by TRUMP in any given time window.

3.1 THE 1-D NODE GENERATOR

The 1-D node generator, TCY1, was used in this study for those cases where cylindrical coordinates were required. The 2-dimensional node generator, discussed in the next section, was only applicable for rectangular regions. The input data to the TCY1 generator is very minimal, making it a convenient tool for rapid analyses and parameter studies of one-dimensional problems. The geometry that can be treated with TCY1 is shown in Figure 18. As with all node generators a material specification grid is overlayed on top of the computational grid so that different material layers can be specified. The node number system employed by the program is also shown in Figure 18.

3.2 THE 2-D NODE GENERATOR

The 2-D node generator, TODXY, was used in the previous study (1) and has been used in the current work on most of the problems. For the present purposes it was extended to include a corner radius and an option for symmetry through the corner radius. Figure 19 shows the various configurations that can be analyzed with the TODXY input data generator. The boundary conditions on each of the four sides can be specified as either convective or insulating. The TODXY generator assumes a certain numbering scheme for the nodes. This scheme is shown in Figure 20 for a typical case. When TRUMP input data blocks other than 4, 5, and 6 are to be specified, the numbering system defined in Figure 20 has to be adhered to. The node numbering scheme has to be known also for the post-processor program, TMPPOST, to retrieve from the results file the temperature histories of selected nodes.

3.3 THE 3-D NODE GENERATOR

The three-dimensional node generator, THREED, was specifically written for the folded ammunition geometry. The geometry and node nomenclature are shown in Figure 21. Because only a few rounds of firing were of interest the boundary conditions removed from the bore surface and the powder region were assumed to be adiabatic. This made possible the symmetry approximation shown in Figure 21. The node generator sets up all of the node characteristics in a two-dimensional plane of unit thickness. The three-dimensional geometry is then set up by stacking any number of these slices, each with a specified thickness. Each axial wafer is associated with a different set of bulk temperatures and heat transfer coefficients.

3.4 THE ROTATING BAND MODEL

This section describes a thermal model that evaluates the temperature histories in a simplified geometry of the interaction of the rotating band and the gun tube. The present model basically considers one surface sliding over another. An attempt to solve a similar problem analytically was made by Chen (7), but it was found that the convergence of temperature solutions were too slow to give accurate results. The present model is based on a numerical solution of the applicable equations and boundary conditions by making use of the existing heat transfer code TRUMP. By making certain modifications to the program the problem of one surface sliding over another can be simulated very nicely. The model is shown schematically in Figure 22.

The gun tube is represented by a set of nodes equally spaced along the length of the tube. The rotating band is represented similarly but with fewer nodes. The interface frictional heating is modelled by a zero-volume heat generating node attached to the sliding surface. The heating rate can be specified as a function of time, distance, or temperature. For the present cases it is assumed constant. The modifications made to TRUMP were with respect to the definition of the six thermal connections in the interface region shown in Figure 22. These are called dynamic connections. As can be seen from Figure 23 the connections between node 1001 and 1 change as a function of time, as detailed in Figure 24. When the interface area, A, becomes zero, i.e., node 1001 has passed node 1 completely, the node terminal points in the gun tube region of each of the dynamic connections is redefined. For example, for times t, less than $\Delta X/V$, where ΔX is the mesh spacing in the longitudinal direction and V the velocity of the sliding surface, the gun tube node terminal point for connection (1) is 1, but when $\Delta X/V < t < 2\Delta X/V$ this terminal point is 2.

The ROTBAND node generator was written to calculate the node and connection data for the configuration shown in Figure 22. In addition TRUMP was modified to include a subroutine, DINAM, that keeps track of the dynamic connections. The results of a few calculations with this model are discussed in Section 4.

Section 4

RESULTS

This section presents results and analyses of various calculations made with the models and tools discussed in Section 3.

4.1 PEAK TEMPERATURE ANALYSES WITH NEW BOUNDARY CONDITIONS

Surface temperature profiles were generated in the same manner as in the previous work [1] using the heat transfer coefficients and fluid bulk temperature data provided by BRL for the new propellant [2]. The program HTSORT, which processes the raw boundary data for use in TRUMP, was modified to accept the format of the new data sets.

With the new boundary conditions on file, 1-D analysis for several locations along the length of the guntube were performed. The results of these analyses, for steel and brass-covered steel, are presented in Figure 25. Peak surface temperatures are shown as a function of distance along the guntube bore. The curve identified as "brass" considers a brass layer of thickness 1/32" on guntube steel. The curve identified as "steel" considers guntube steel only. As may be noted several maxima exist in this profile. These are due to the given boundary conditions. The cause of the variation in the boundary condition data is not known. The time dependency of the surface temperature at the location where it becomes maximum, location 15, is shown in Figure 26 in addition to the profiles of the two adjacent locations. The profile is very similar to that of the previous studies. Peak surface temperatures in the present study are much lower than those computed in Reference 1. This can be traced to the fact that the bulk fluid temperatures and corresponding heat transfer coefficients are presently lower than those of Reference 1. For these same locations, 14, 15, and 16, the temperature profiles into the wall are plotted in Figure 27 at the time the surface temperature has reached its maximum. These results again show that for a single round of firing the thermally active region in the guntube is less than 1 mm thick.

Temperature profiles for the corner region, shown by an "*" in Figure 1, are given in Figure 28. These profiles are for the same case as the one shown in Figure 25 of Reference 1. The peak surface temperature increases markedly in the corner when this region is maintained sharp. As soon as a corner radius is provided the peak surface temperatures change considerably. Using the "radius" option in TODXY several calculations were performed for different corner radii. The results are displayed in Figure 29. As noted, even a very small corner radius is effective in reducing the peak surface temperature during a single round of firing.

4.2 GUNTUBE COATINGS AND THERMAL PROPERTY SENSITIVITY

Sensitivity analyses were performed to evaluate the effect of uncertainties in the calculated peak surface temperatures due to the inaccurate knowledge of the thermal properties of the materials involved. A simple parametric study was performed using the Reference 1-D geometry and the boundary conditions at the location that provided the maximum surface temperature, location 15. The thermal properties, specific heat and thermal conductivity, were varied ±20% around the nominal value and the peak surface temperature computed. The results are displayed in Table 3. As may be noted the temperatures do not deviate significantly from the mean. Examining the results one may use a rough rule of thumb that states that a 1% change in the thermal property, either specific heat or thermal conductivity produces a 0.4% change in the peak surface temperature rise.

The sensitivity of the peak surface temperature due to coatings on guntube steel are shown in Table 4, where three thicknesses—1, 3, and 6 mils—were analyzed for three different coating materials—chromium, tungsten, and molybdenum. As may be noted the thicker the coating the lower the surface temperature. This is a result of the fact that the thermal diffusivity of these coating materials is higher than that of gun steel. It should also be noted that the differences from coating to coating are very slight.

4.3 MULTIPLE FIRING RESULTS

In the previous study (1) results were reported for a 1-D multiple firing case. A similar case was run with the new set of boundary conditions. The multiple firing model recycles a table of time-dependent heat transfer coefficients and bulk fluid temperatures with a cycle time that depends on the last entry in the table. For example, if the last value in the time table is 0.1 sec, then a burst of 600 rounds per minute is simulated. The version of TRUMP that has been used in all of the calculations presented in this report accepts a table with a maximum of twelve entries. It is relatively easy to change the table length with the DIMENS program, but this was found not to be necessary. The boundary condition set at location 15 was approximated by a table of ten entries. The resulting maximum surface temperature when used with the 1-D geometry was 379 ^{o}C, as compared with a temperature of 376 ^{o}C when the full set of values as given by Reference 2 was used. Hence, the short table was deemed adequate for the multiple firing case. Figure 30 shows the surface temperature history over several cycles. This case can only be taken out to several cycles before the assumed boundary conditions away from the surface start distorting the results. This calculation basically serves to checkout the condition to be employed in the 3-D multiple firing problem.

Table 3. Material Property Sensitivity Analysis Results

Multiplier to Thermal Properties		Peak Surface Temperature ^{o}C	Percent change from Nominal*
Specific Heat	Thermal Conductivity		
0.8	0.8	422.8	19.3
1.0	0.8	388.7	9.2
1.2	0.8	363.3	1.7
1.0	1.0	357.6	0.0
0.8	1.2	363.7	1.8
1.0	1.2	333.8	-7.0
1.2	1.2	311.6	-13.6

*Calculated as $(T-T_r)/(T_r-20) \times 100$; T_r is the temperature when the multipliers are 1.0.

Table 4. Peak Surface Temperatures (^{o}C) with Different Coatings

Coating Thickness (mils)	Coating Type		
	Tungsten	Molybdenum	Chromium
1	519	520	519
3	480	483	483
6	438	444	452

The three-dimensional model is shown in Figure 21 where the 3rd dimension is achieved by stacking three slices of equal thickness on top of each other. The boundaries at the top and bottom of the stack were assumed to be adiabatic. This model provides a larger volume (heat sink) around the chamber regions, thus more nearly characterizing the heat capacity of the surrounding material. Nodes at the surface of the chamber regions were assigned the following boundary conditions from Reference 2:

	Projectile Chamber	Powder Chamber
Top Level	Loc. 15	Loc. 13
Mid Level	16	12
Bot Level	17	11

The boundary condition data were reduced to 12-point tables for use in TRUMP without any significant loss in accuracy, as previously described. Figure 31 shows peak temperature histories of surface nodes 5001 and 5005 (see Figure 21 for nomenclature) for four firings. Also shown is the corresponding 1-D temperature history for location 15. The effects of the improved modeling are readily observed. The increased volume allows circumferential heat flow away from the chamber surface area thus decreasing the surface temperature. Lower projectile chamber surface temperatures are also observed at nodes away from the web area (node 5005). Figure 32 shows the temperature distribution in the web at four time periods corresponding to the instant of maximum surface temperature of node 5001. One can observe the 3-D effects; the inner region or web temperature increases with each round fired.

4.4 THE ROTATING BAND RESULTS

The rotating band model discussed in Section 3.4 was used to generate the results shown in Figures 33 through 35. It should be remembered that the model is a first attempt at evaluating the interaction of one surface sliding over another on the temperature distributions. The model in its present form does not represent the actual environment of the rotating band because of the following inherent assumptions. The major assumptions of the model are: 1) the heat generated by friction is constant with time; 2) the velocity of the sliding surface is constant; 3) the boundary conditions on the sliding and stationary surfaces are adiabatic; 4) the materials are not allowed to melt; 5) the geometry is semi-infinite rectangular. The order in which the assumptions are listed above also reflects their relative importance on the calculated temperatures. All of these assumptions can be relaxed without any major difficulties. They require, however, additional effort which is beyond the scope of the present study.

The present results were calculated with the geometry and node structure shown in Figure 22. The length of the sliding surface was taken as 1 cm and its thickness and that of the stationary surface

were taken as 0.1 cm. The heat generated by the sliding surface was estimated from the data given by Montgomery (8). The rate of heat generated by sliding is equal to the product of the coefficient of friction, the bearing pressure, and the slider velocity. This product is denoted by fPV, and its value represents a heat flux. The results reported in the present study are based on a value of 4.2×10^8 watt/m^2 (0.2×10^5 ft-lb_f/in^2-sec.)

Figure 33 shows how the maximum temperatures at different locations vary as a function of the sliding surface velocity. As expected, the higher the velocity the lower the temperature. The node numbers identified on the curves are with reference to Figure 22. As may be noted, the temperatures of node number 4 are larger than those of node number 1 or 2 because of its larger contact time with the sliding surface. Also, node 6 temperatures are larger than node 4 temperatures because the sliding surface temperature at the interface is higher, resulting in higher heat flow. Figure 34 shows temperature distributions along the stationary surface for two different times and, hence, two different sliding surface positions. Note the decaying temperature behind the sliding surface and the colocation of the peak temperature with the rear position of the sliding surface. Figure 35 shows the temperature histories of three locations on the sliding surface. Note the rapid rise and the apparent leveling off of the temperatures. Eventually, under the conditions specified, a steady temperature distribution can be expected.

We would like to iterate that these results are preliminary. Further parameter studies need to be conducted to determine whether the node structure is fine enough. For example, it was found from other calculations with the same geometry and dimensions, that subdividing the sliding and stationary surfaces into ten rather than three intervals in the vertical direction reduces the temperatures somewhat. The present calculations show however that TRUMP can be adapted to sliding surface problems.

Section 5

CONCLUSIONS AND RECOMMENDATIONS

The analyses and results discussed in this report are applicable to a variety of heat transfer problems in gun tubes. They also confirm the usefulness of TRUMP, the heat transfer computer code used in all of the calculations, for solving problems of this nature. The conclusion of the various analyses performed here can be summarized as follows. The new boundary conditions (2) result in significantly lower surface temperatures than those of the previous study (1), that is, 377 ^{o}C versus 660 ^{o}C when the inside surface is brass and 540 ^{o}C versus 1003 ^{o}C when the inside surface is gun steel. For the current set of boundary conditions the effect of uncertainties in the thermal properties of the materials can be considered moderate. The results show that a 1% change in either specific heat or thermal conductivity produces approximately a 0.4% change in the peak surface temperature rise. The effect on the peak surface temperature of the three surface coatings-tungsten, molybdenum, and chromium-is that they tend to lower the surface temperature slightly and that this drop becomes larger as the coating thickness increases. Differences from coating to coating are very slight. The three-dimensional multiple firing model shows that three-dimensional effects are important when more than a single round of firing is considered. The rotating band model, simulated by one surface sliding over another and described in this report, worked out very well. All major features of the problem can be simulated with TRUMP. The analyses performed in this report with the model do not represent the actual environment of the rotating band because of a number of inherent assumptions. These assumptions, however, can be relaxed quite readily with a little more development work.

The results presented in this report suggest a number of recommendations for further work. If further modelling is to be performed with TRUMP it would be very useful to rework the code so that it is more efficient to run and more flexible. The TRUMP code has been in use and continuously improved since 1965. Because of earlier programming practices, the program consists of a small number of large routines as opposed to many small modules, resulting in much inefficiency. All the routines and programs discussed in this report can be merged readily into a modular system.

The three-dimensional multiple firing model can be improved by providing other than an adiabatic boundary condition at the bottom of the stack. Furthermore, the model can be extended further away from the gun tube surface and be provided with external boundary conditions.

The rotating band model has been shown to be feasible with TRUMP. Extensions in this area include making the heating rate and band velocity time-dependent, accounting for the melting effects of the materials, using a cylindrical geometry, and adding heat transfer coefficient boundary conditions.

LIST OF REFERENCES

1. P.L. Versteegen, F.D. Varcolik, N.E. Banks, G.J. Klem, "A Heat Transfer Study in Folded Ammunition Gun Tube Chambers," BRL-CR-342, July 1977. (AD #A043280)

2. G.J. Klem, private communication (data of March 3, 1977).

3. Y.S. Touloukian, R.W. Powell, C.Y. Ho, P.G. Klaneus, Thermal Conductivity: metallic elements and alloys IFI/Plenum, 1970.

4. Y.S. Touloukian, E.H. Buyco, Thermophysical Properties of Matter V.4 Specific Heat: metallic elements and alloys, IFI/Plenum, 1970.

5. C.Y. Ho, R.W. Powell, Lilley, "Thermal Conductivity of the Elements," Journal of Physics & Chemistry, Ref. Data, V. 3, Supplement 1, 1974.

6. A.L. Edwards, "TRUMP: A Computer Program for Transient and Steady State Temperature Distributions in Multidimensional Systems," LRL Livermore, UCRL-14754 (1972) Rev. 4.

7. Y. Chen, "The Thermal Aspects of the Wear of Plastic Materials Under Very High Contact Pressure and Sliding Velocity," AD A022388, January 1976.

8. R. S. Montgomery, "Friction and Wear at High Sliding Speeds," Wear V. 36, 275-298 (1976).

9. Y. S. Touloukian, et. al., Thermophysical Properties of Matter, Vols. 1 and 4 (1970).

10. T. W. Watson, H.E. Robinson, ASME, J. Heat Transfer, 83(4), 403-408 (1961).

11. W. J. Parker, R.J. Jenkins, C.P. Butler, G.L. Abbott, J. Appl. Phys., 32(9), 1679-1684 (1961).

12. J. H. Awbury, A.R. Challoner, P.R. Pallister, J. Iron Steel Inst. (London), 154(2), 83-111 (1946).

13. L. C. Bailey, Proc. Roy. Soc. (London), A134, 57-76 (1931).

14. C. S. Smith, Trans. Met. Soc. AIME, 89, 84-106 (1930).

15. Von. A. Kussman, H. Wollenberger, Z. Metallkunde, 50, 94-100, (1959).

16. L. D. Armstrong, H. Grayson-Smith, Can. J. Res., A28(1), 51-59 (1950).

17. G. F. Lucks, H.W. Deem, ASTM, Spec. Publ. (227) (1958).

18. R. Hultgren, C. Land, Trans. Met. Soc. AIME, 215(1), 165-166 (1959).

19. F. Krauss, Metallkunde, 49(7), 386-392 (1958).

20. V. A. Kirillin, A.E. Sheind'lin, V. Ya. Chekhonskoi, V.A. Petrov, Zh. Fiz., Khim., 37(10), 2249-2256 (1963).

21. A. Magnus, H. Holzmann, Ann. Physik 5 , 3, 585-613 (1929).

22. Y. A. Kirillin, A.E. Sheind'lin, V. Ya. Chekhonskoi, Teploenerg, 9(2), 63-66 (1962).

23. F. M. Jaeger, E. Rosenbolm, Rec. Trav. Chim., 51, 1-46 (1932).

24. R. E. Taylor, R.A. Finch, USAEC, NAA-6034 (1961).

25. C. W. Kothen, Ph.D. Thesis, OSU, Univ. Microfilms Publ. 52-23697 (1952).

26. F. M. Jaeger, W.A. Veenstra, Rec. Trav. Chim., 53, 677-687 (1934).

27. G. W. Lehman, WADDTR 60-581, 1-19 (1960).

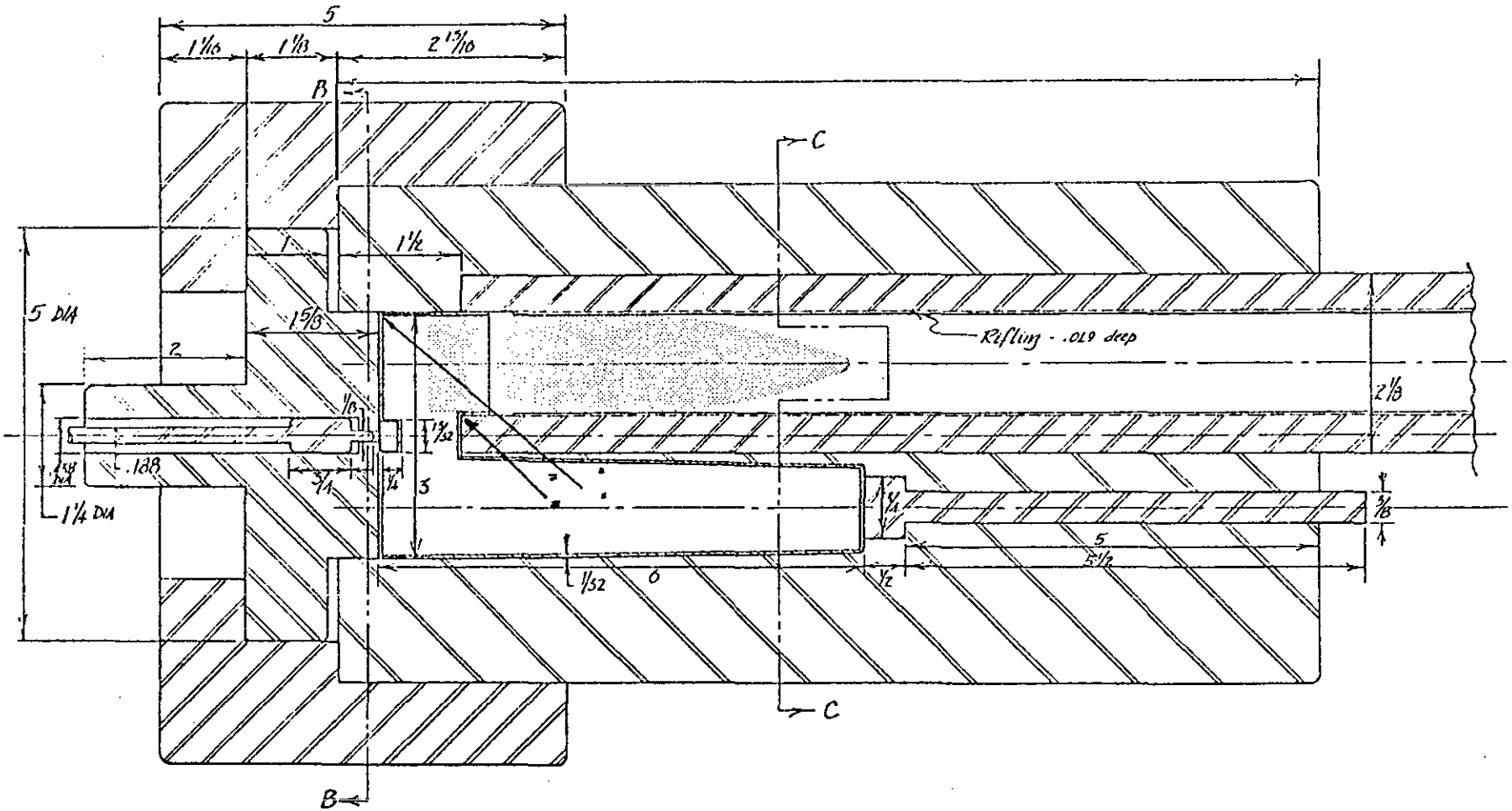

Section A-A

Figure 1. Longitudinal Cross Section of a Folded Ammunition Gun Tube Chamber

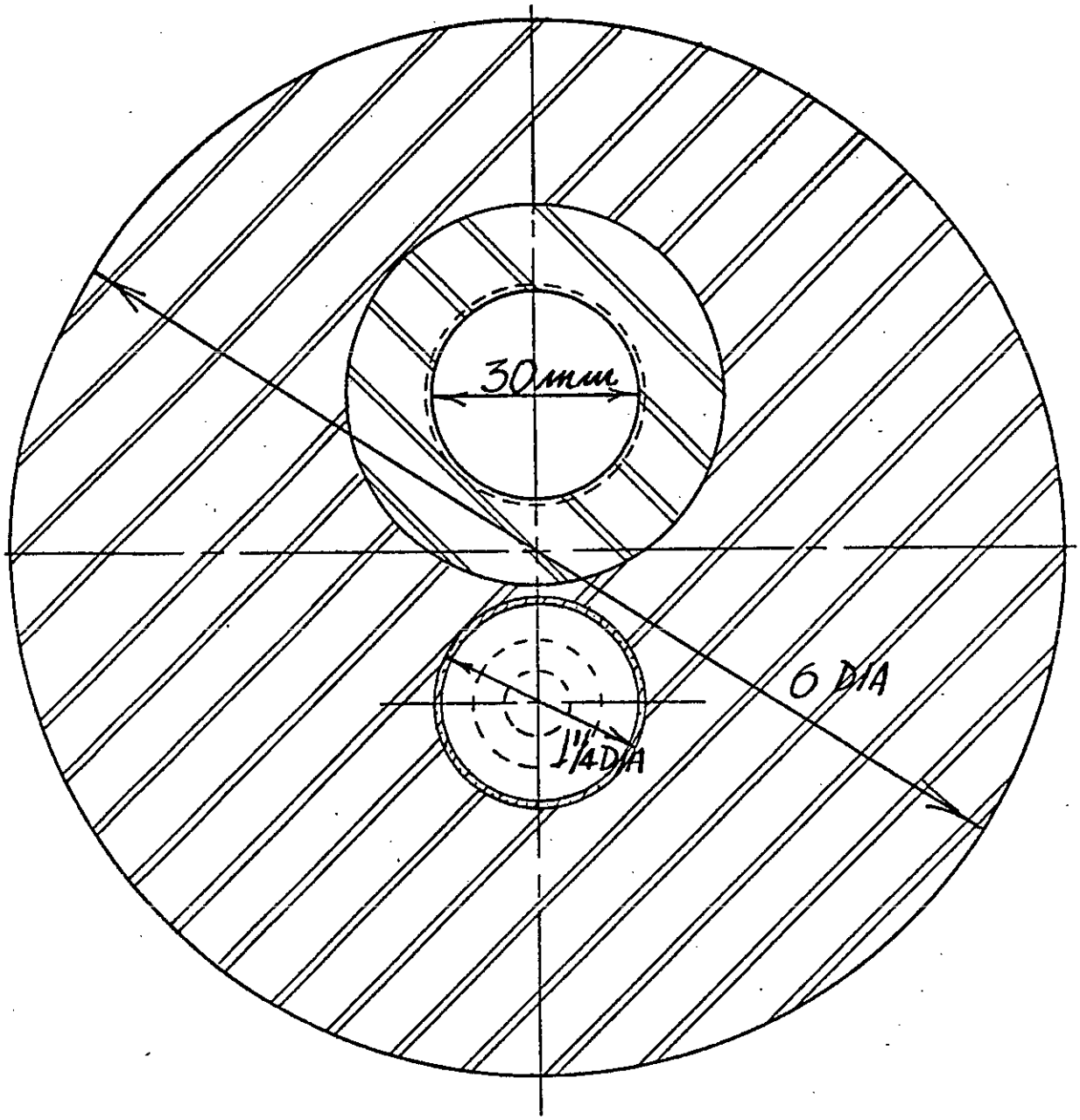

Figure 2. View of Cross Section C-C

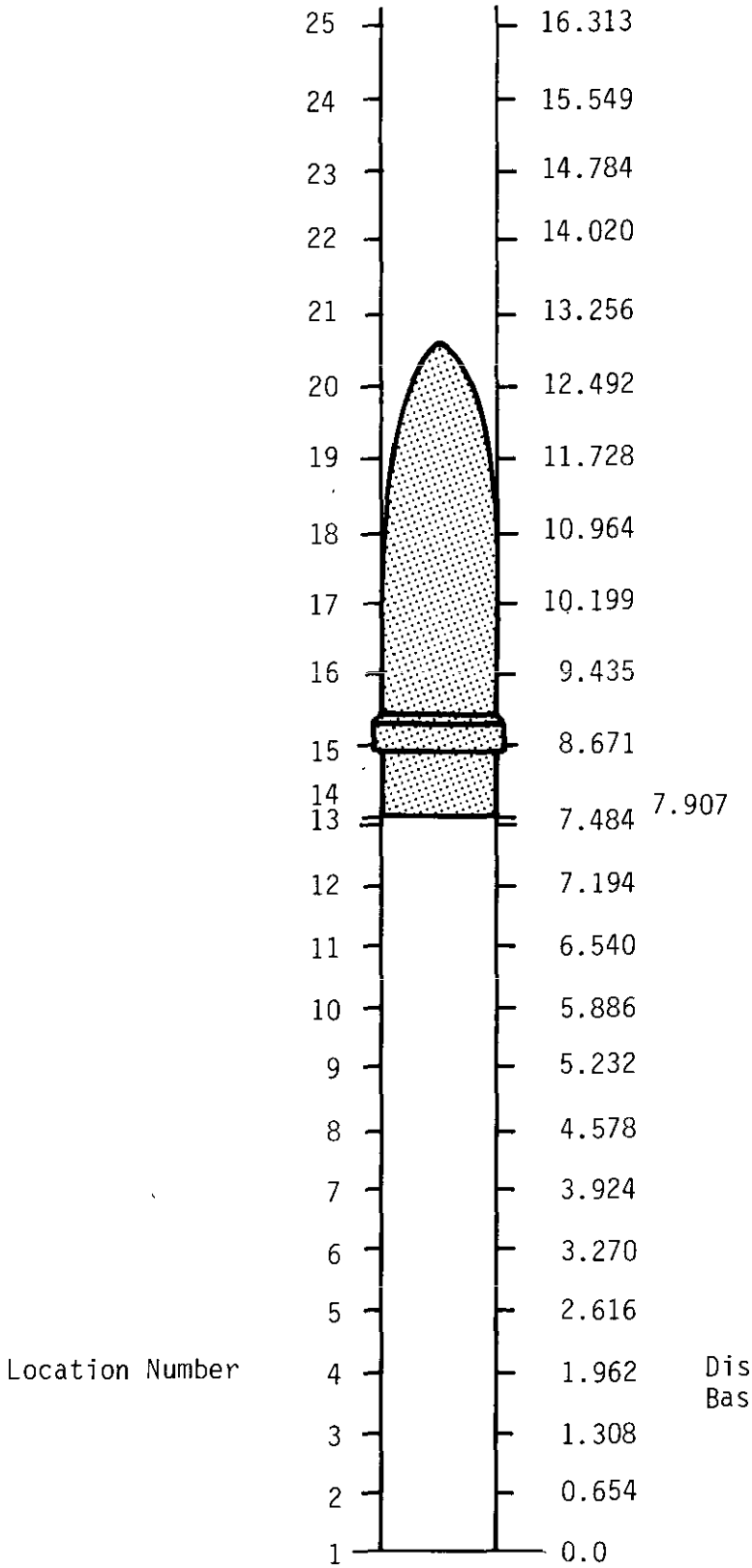

Figure 3. Schematic of the Geometry for which the Boundary Conditions were Generated

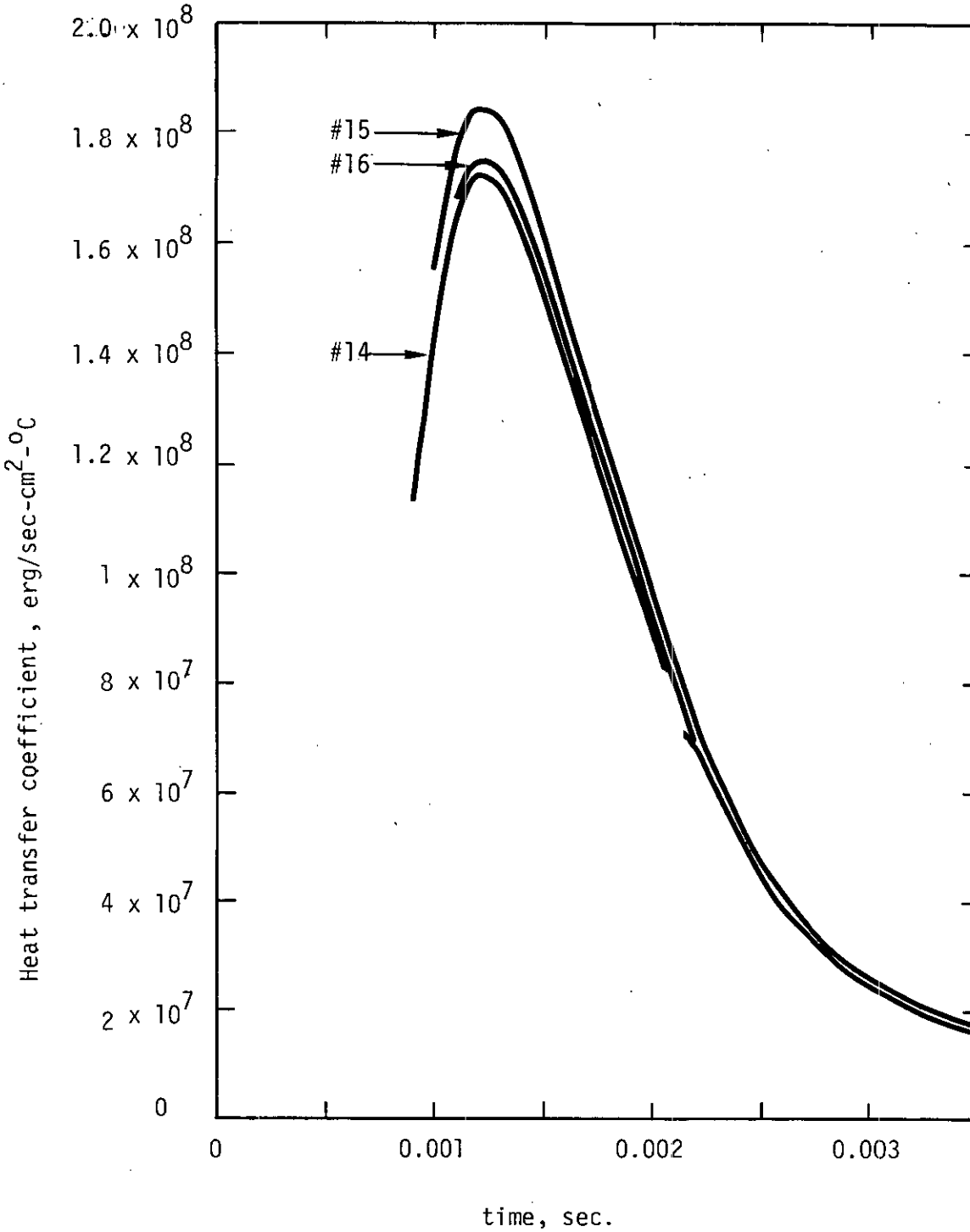

Figure 4. Time Histories of Heat Transfer Coefficients for Locations 14, 15 and 16.

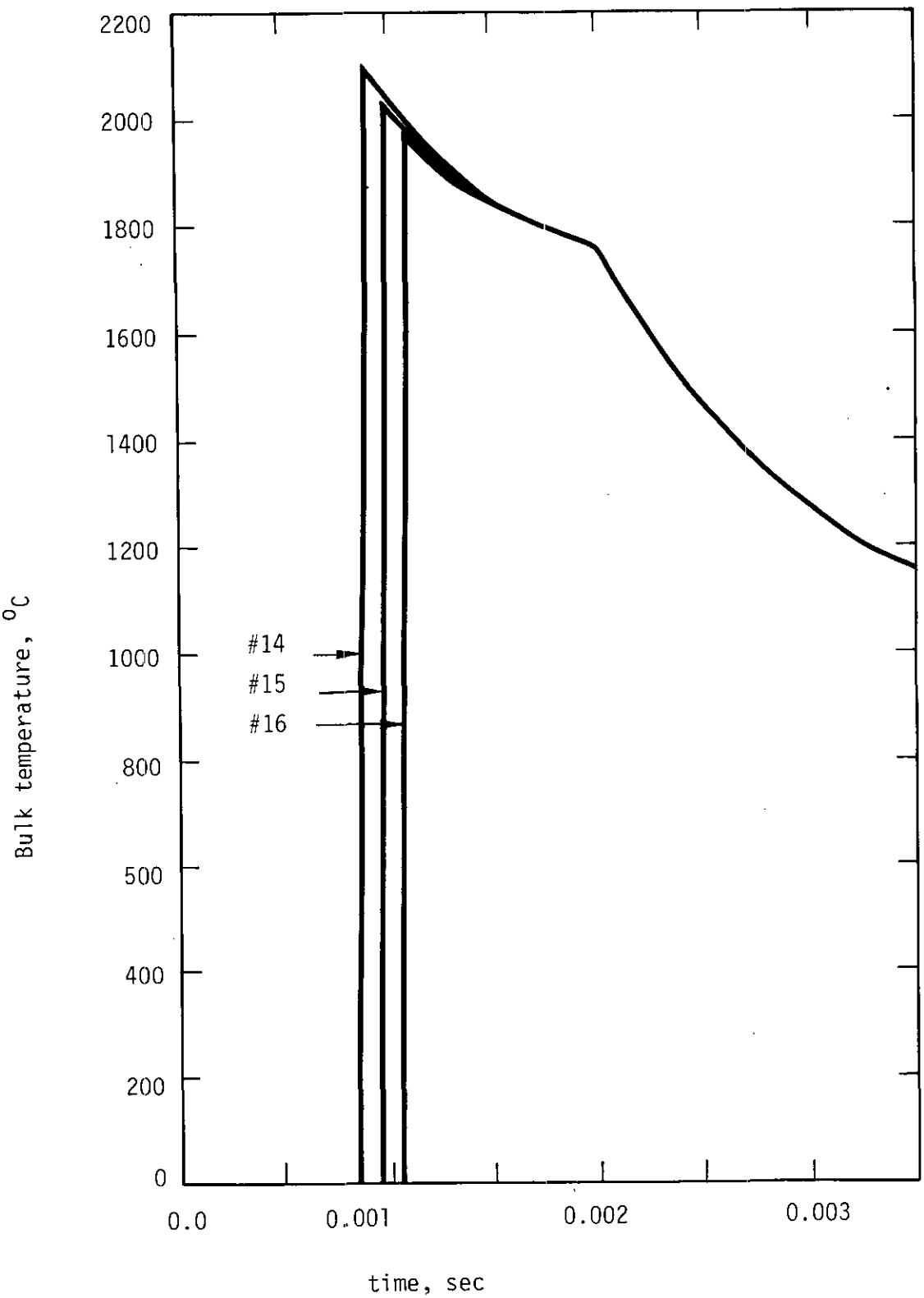

Figure 5. Time Histories of Bulk Fluid Temperatures for Locations 14, 15 and 16.

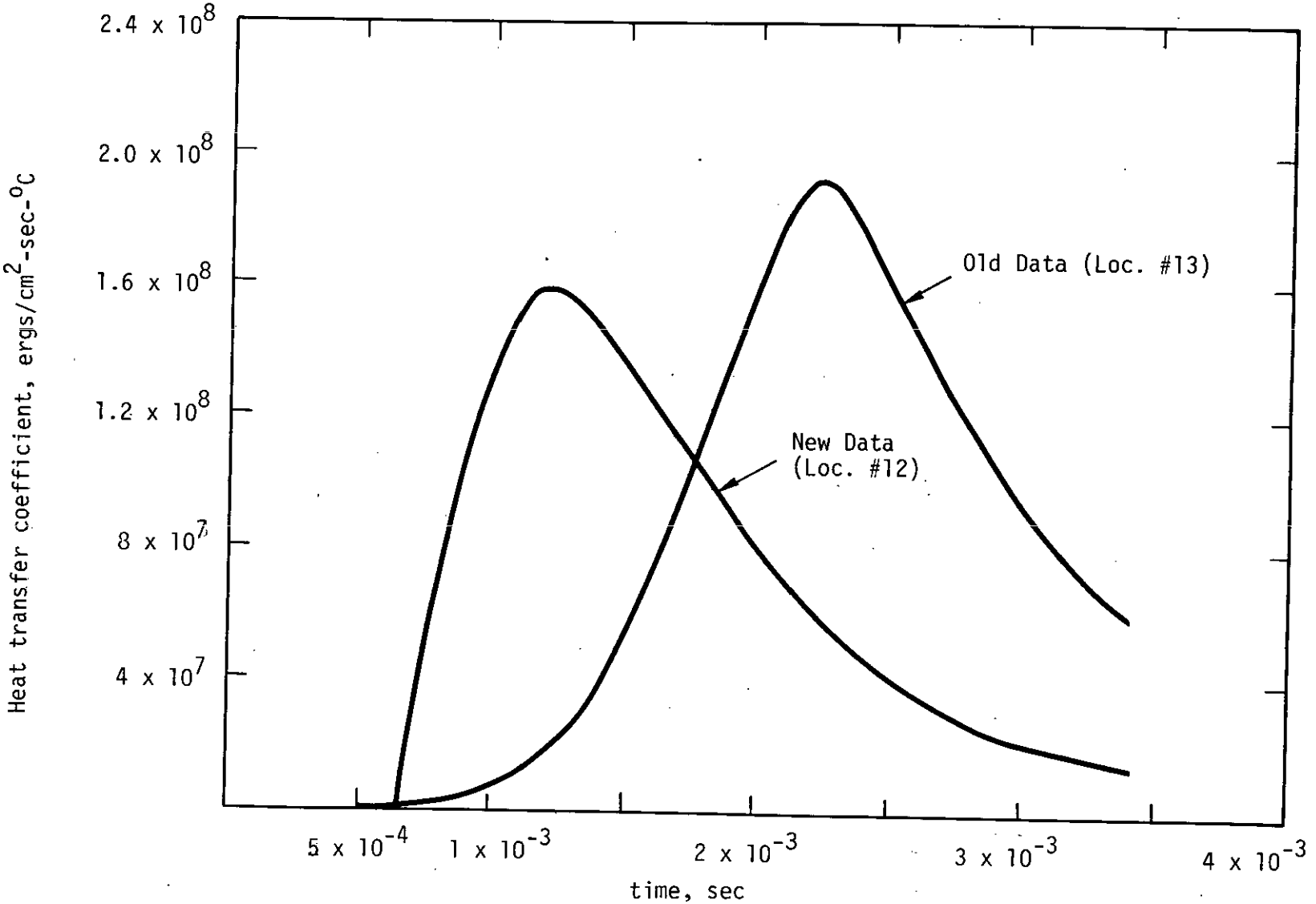

Figure 6. Comparison of Heat Transfer Coefficients at Similar Locations in the Gun Tube

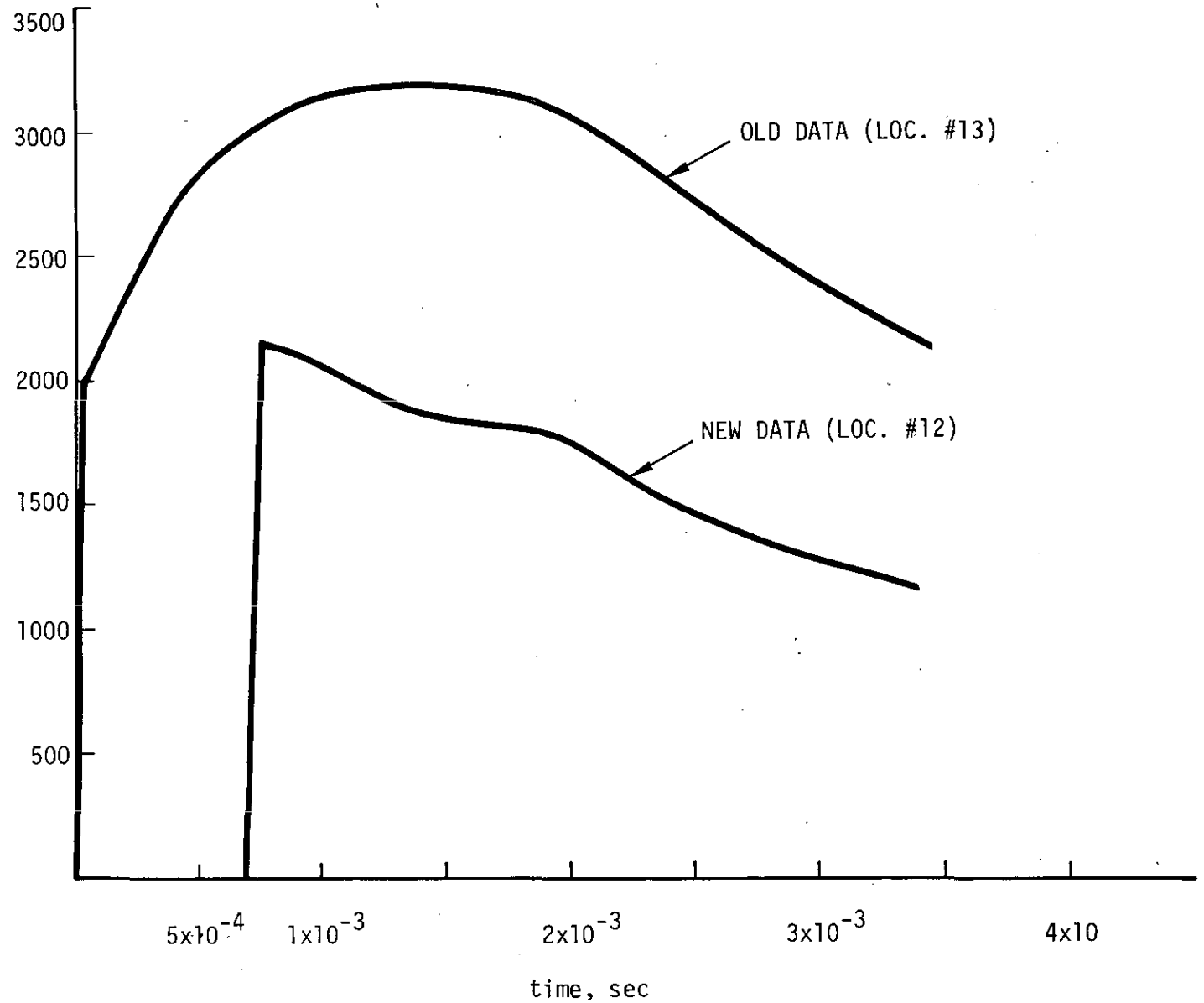

Figure 7. Comparison of Bulk Temperature of Old and New Data at Similar Locationsin the Gun Tube

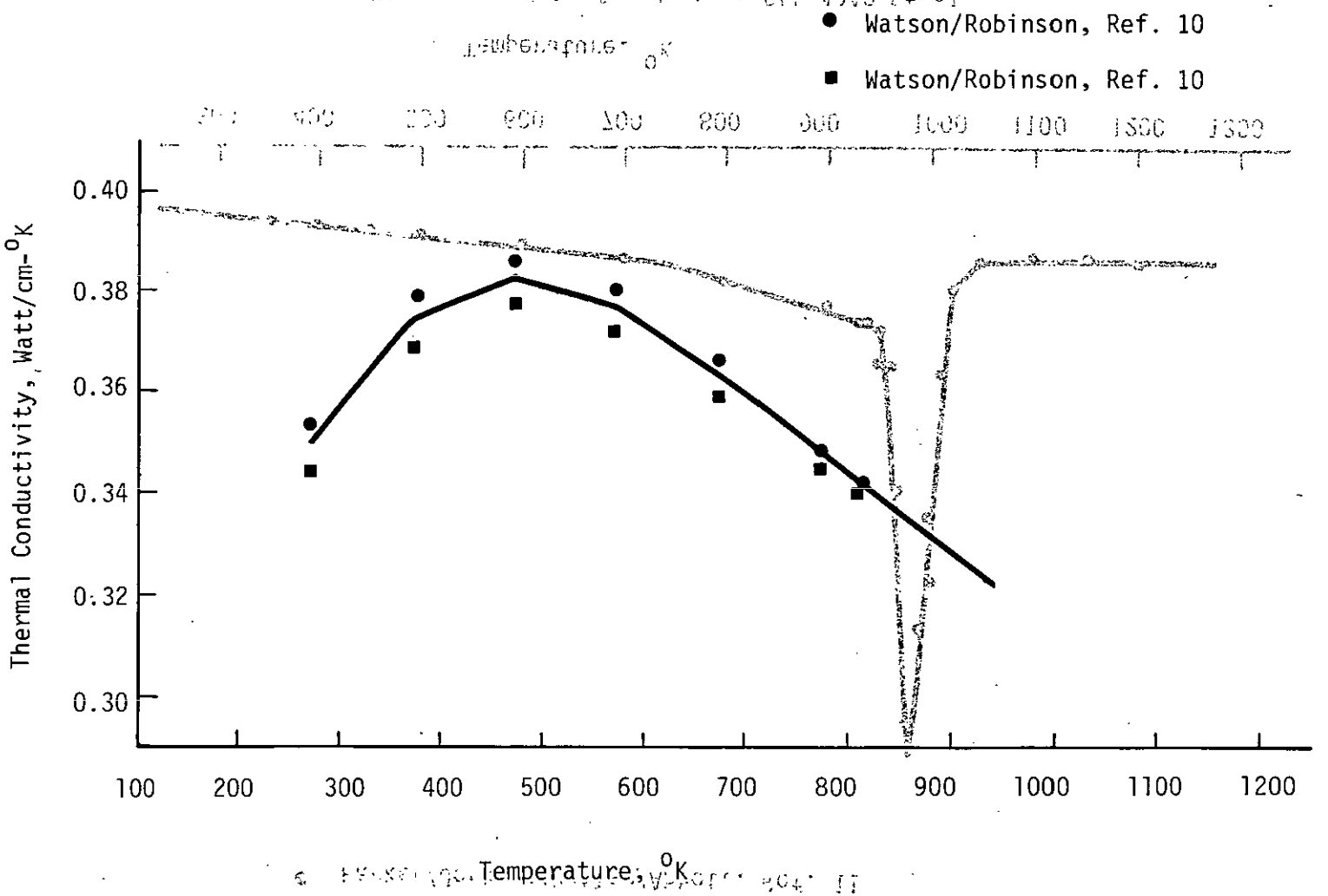

Figure 8. Thermal Conductivity of SAE 4340 Steel

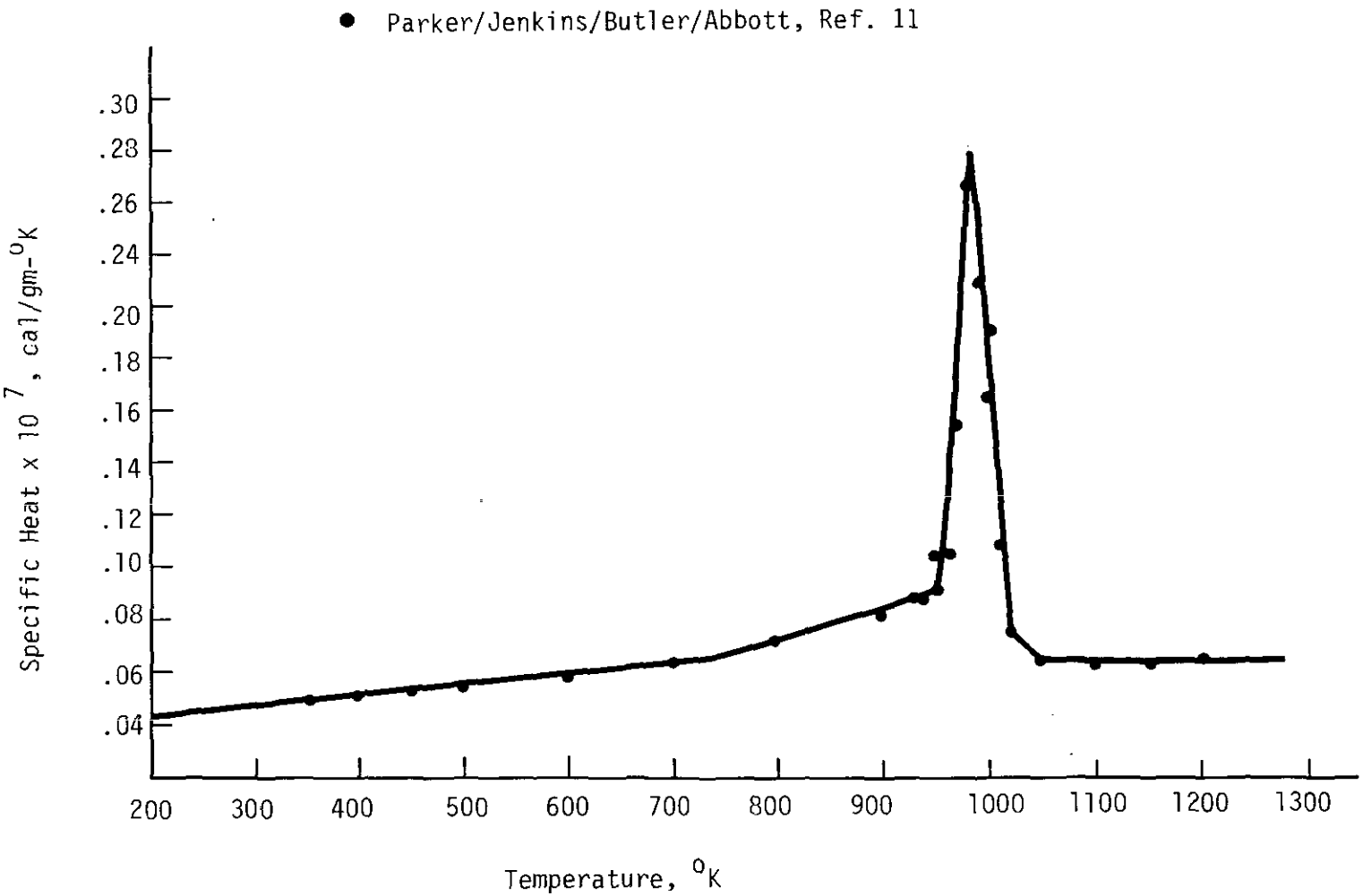

Figure 9. Specific Heat of SAE 4340 Steel

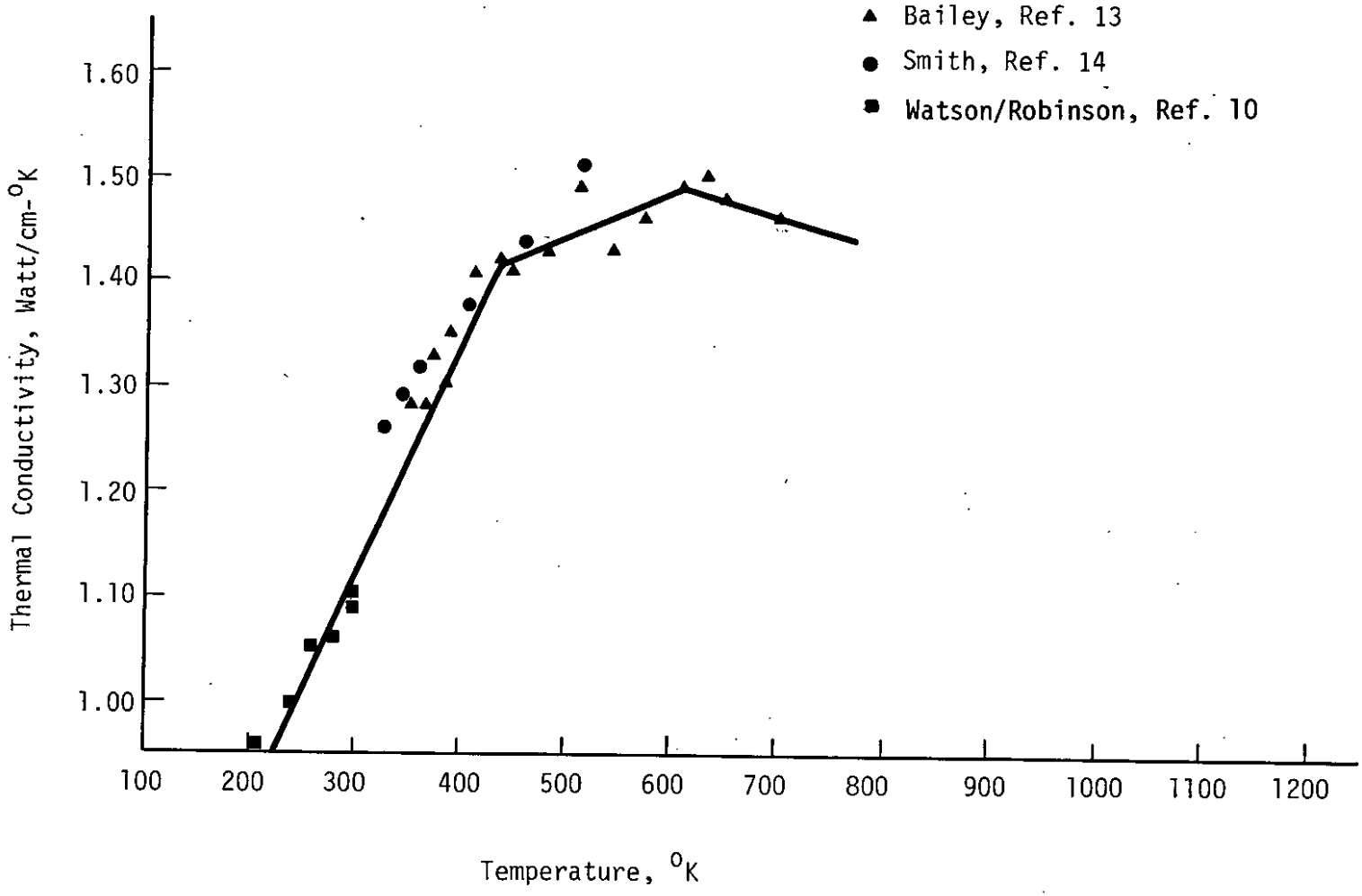

Figure 10. Thermal Conductivity of Cartridge Brass

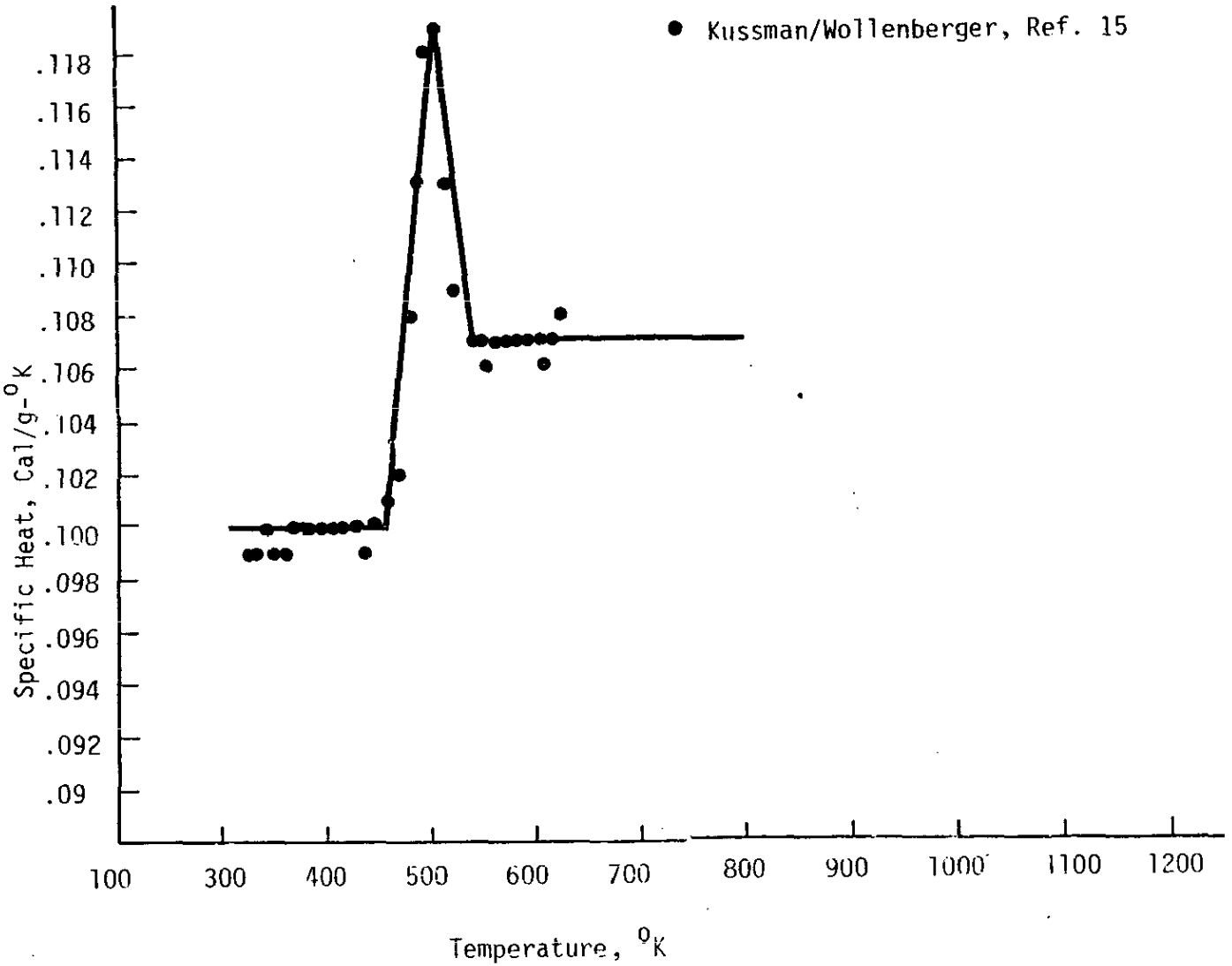

Figure 11. Specific Heat of Cartridge Brass

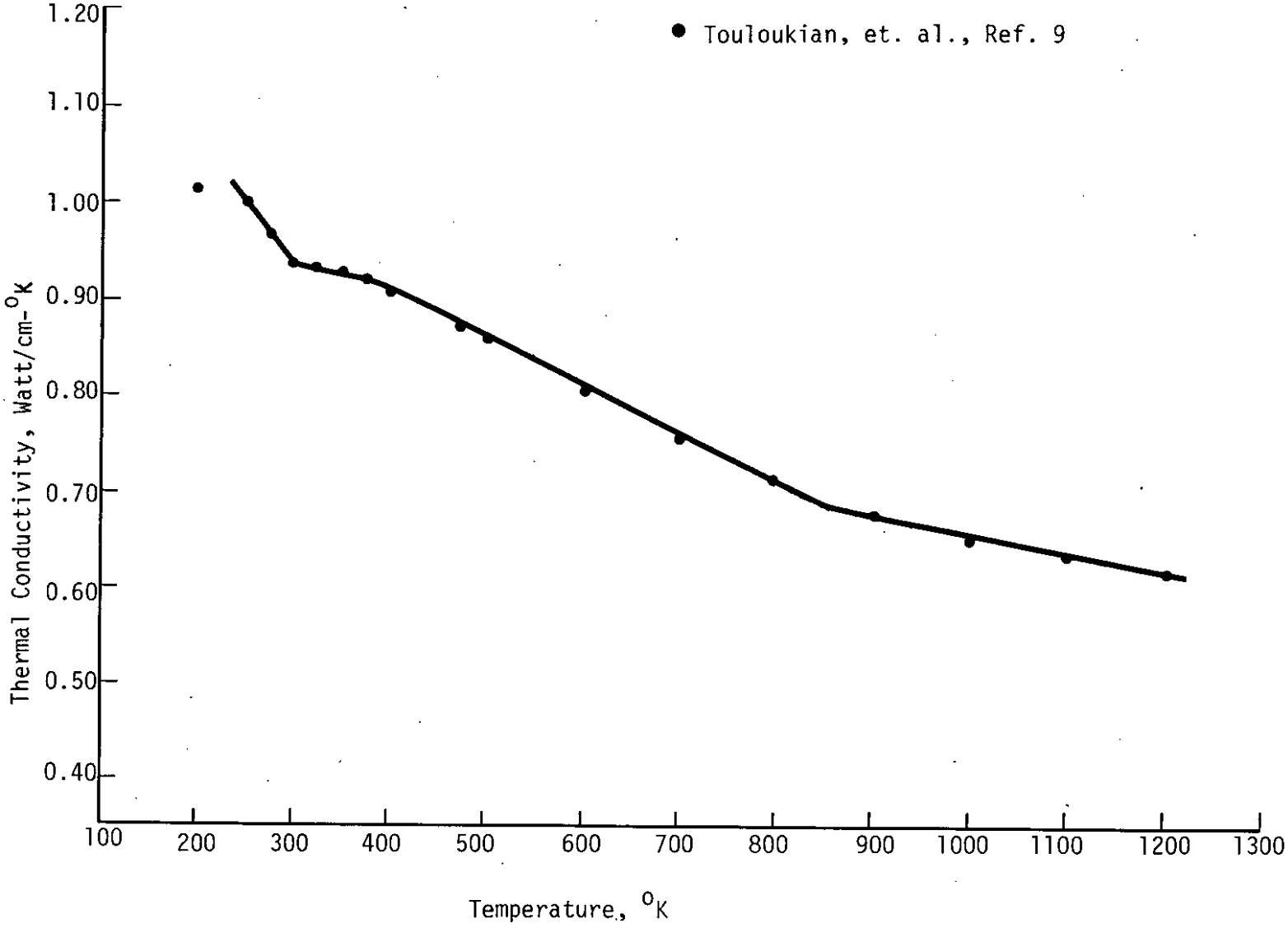

Figure 12. Thermal Conductivity of Chromium

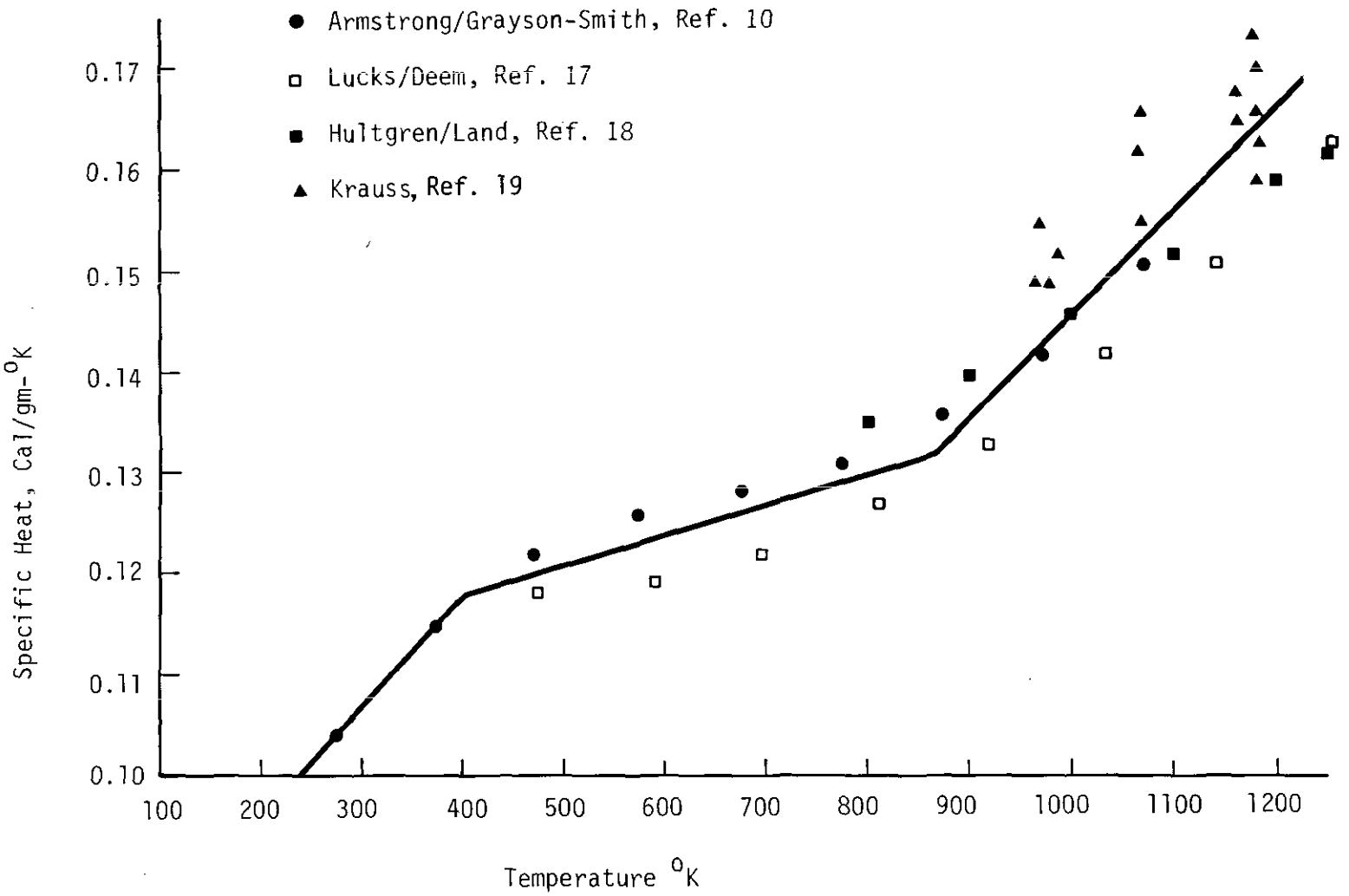

Figure 13. Specific Heat of Chromium

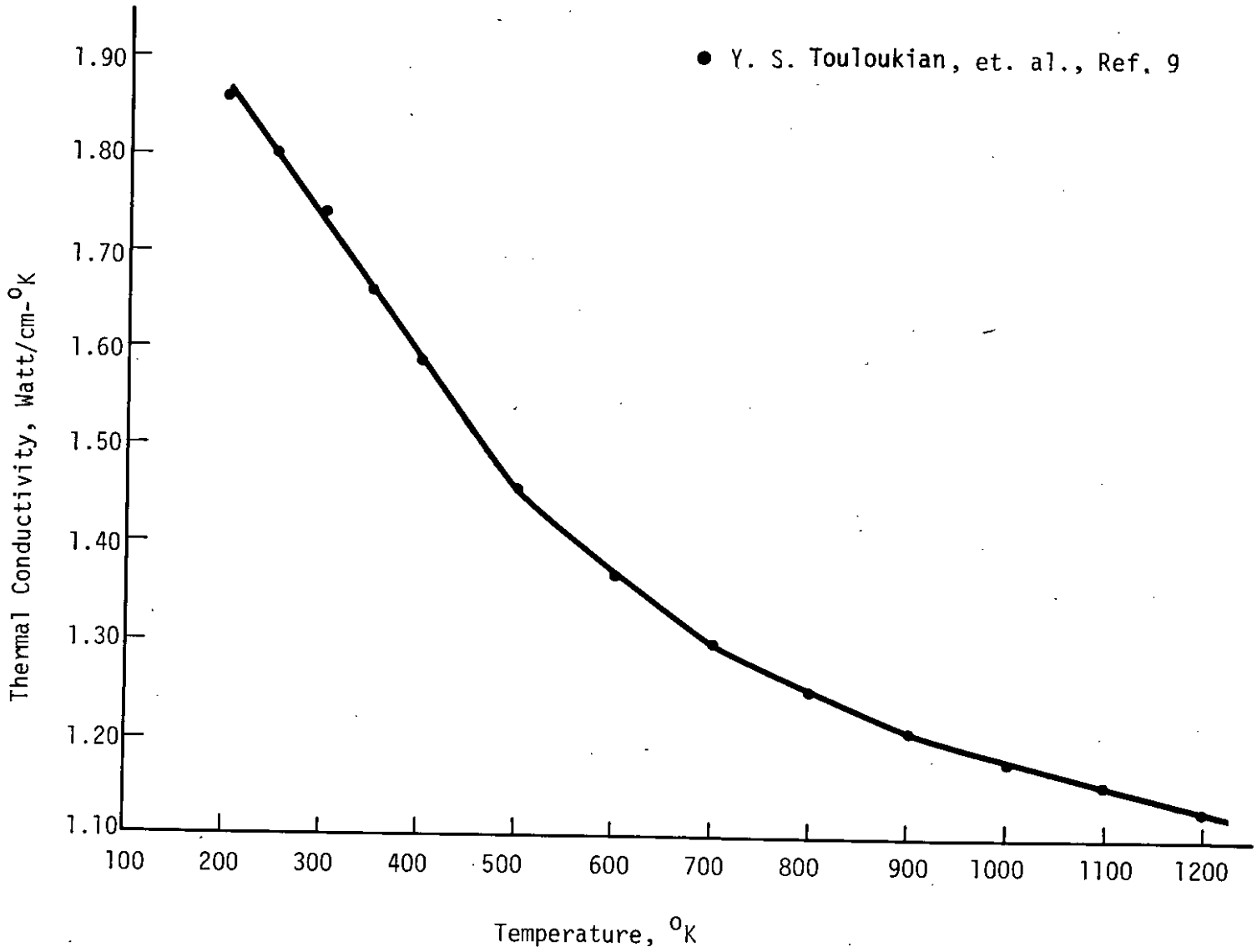

Figure 14. Thermal Conductivity of Tungsten

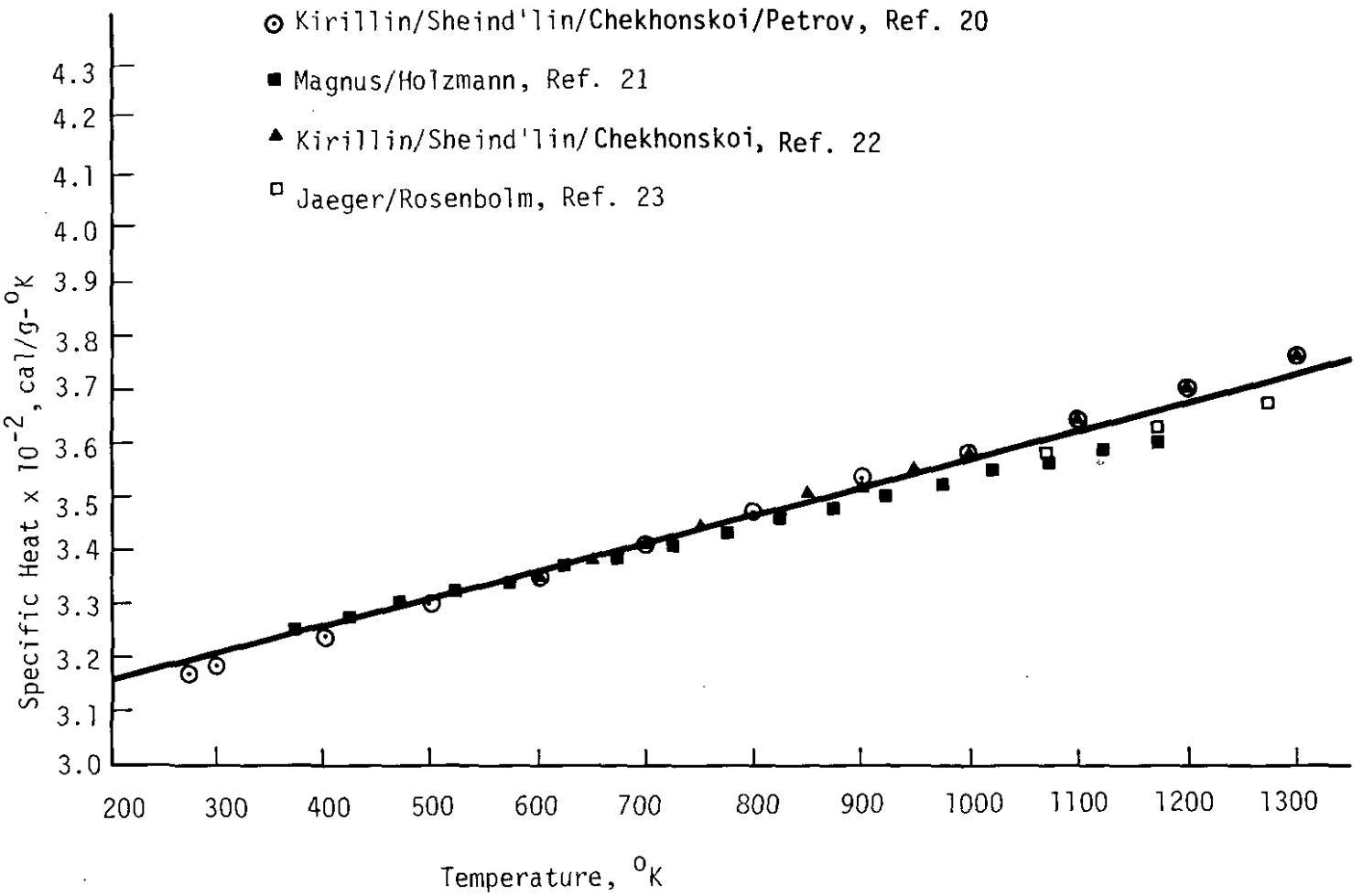

Figure 15. Specific Heat of Tungsten

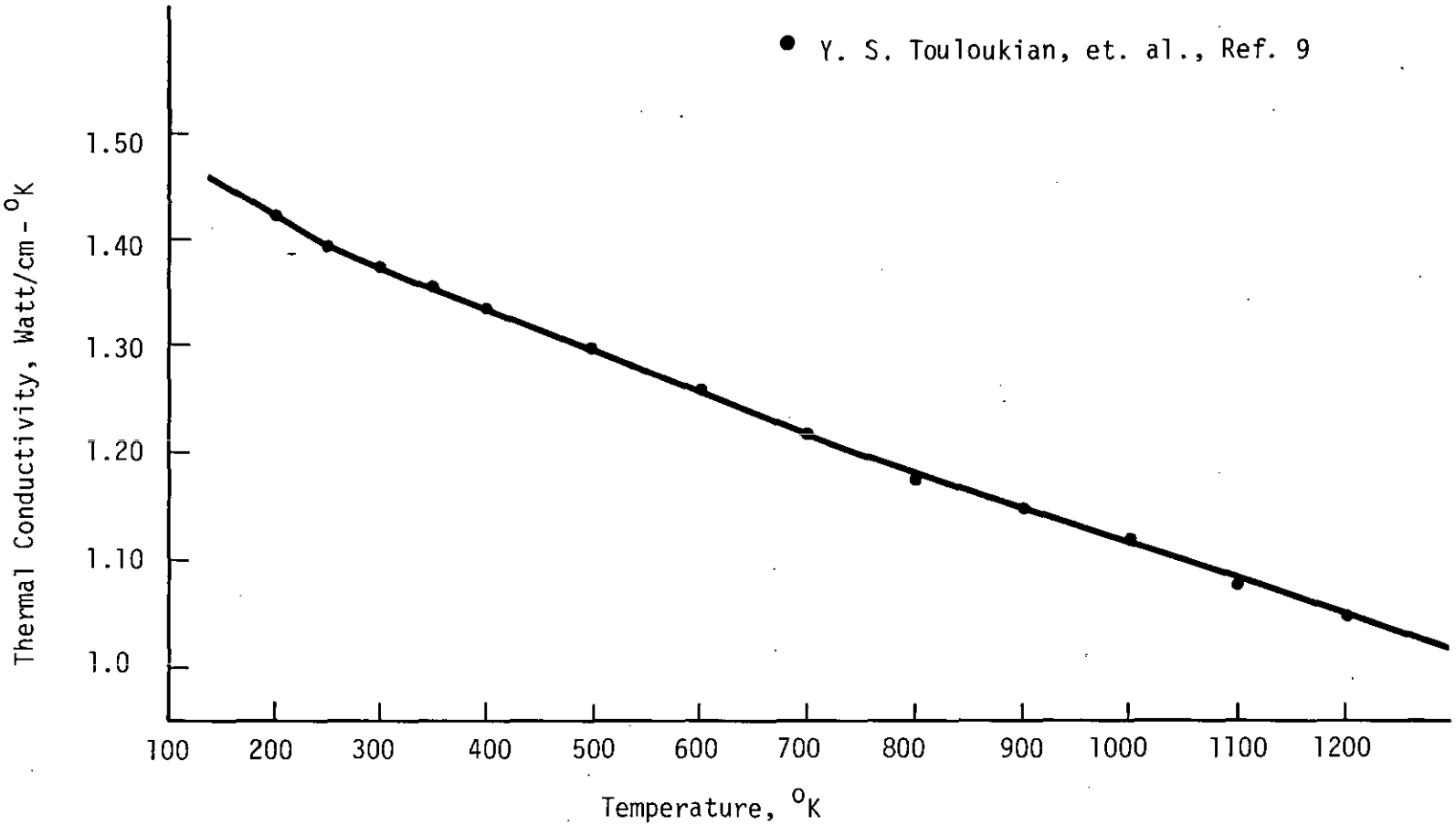

Figure 16. Thermal Conductivity of Molybdenum

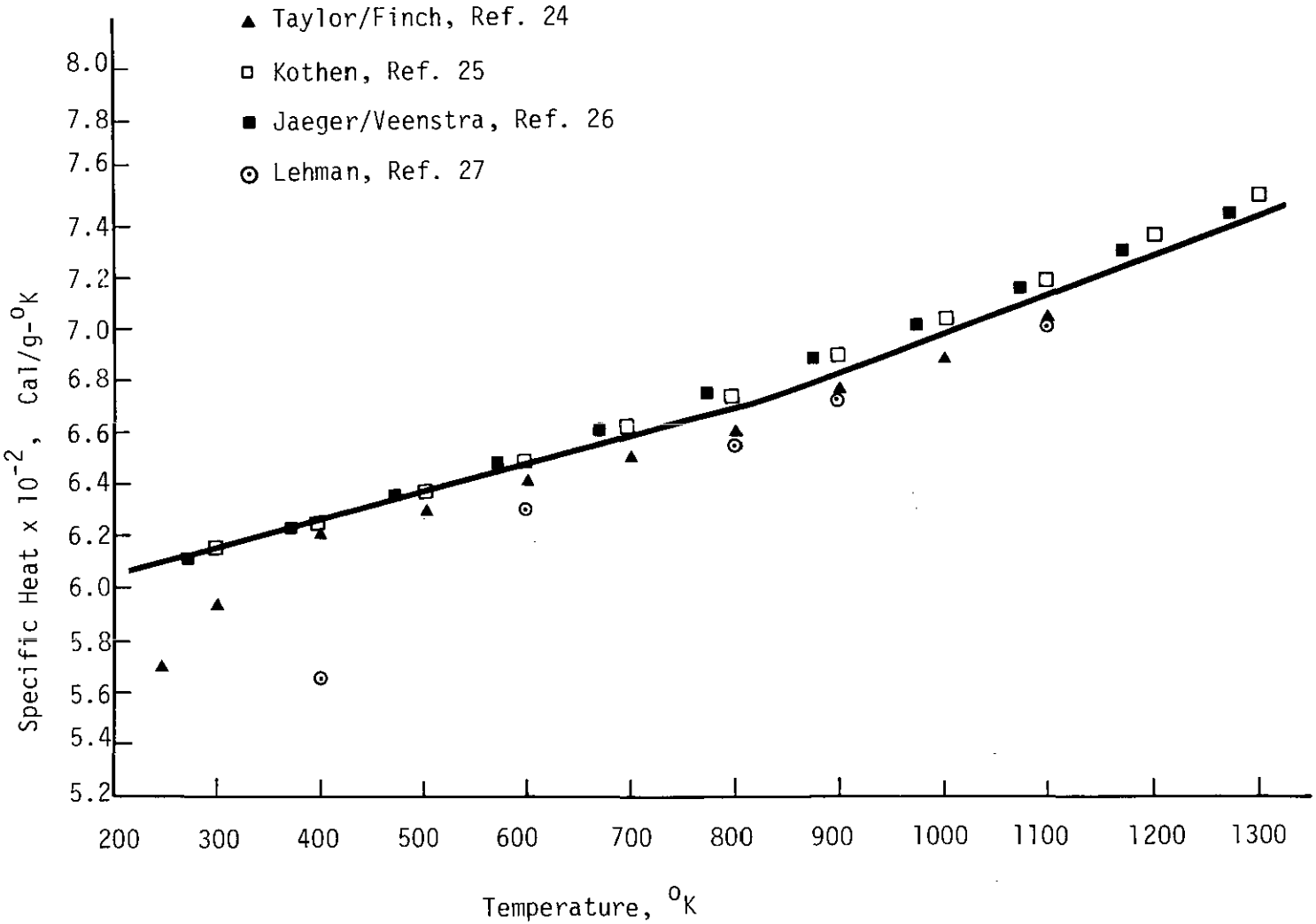

Figure 17. Specific Heat of Molybdenum

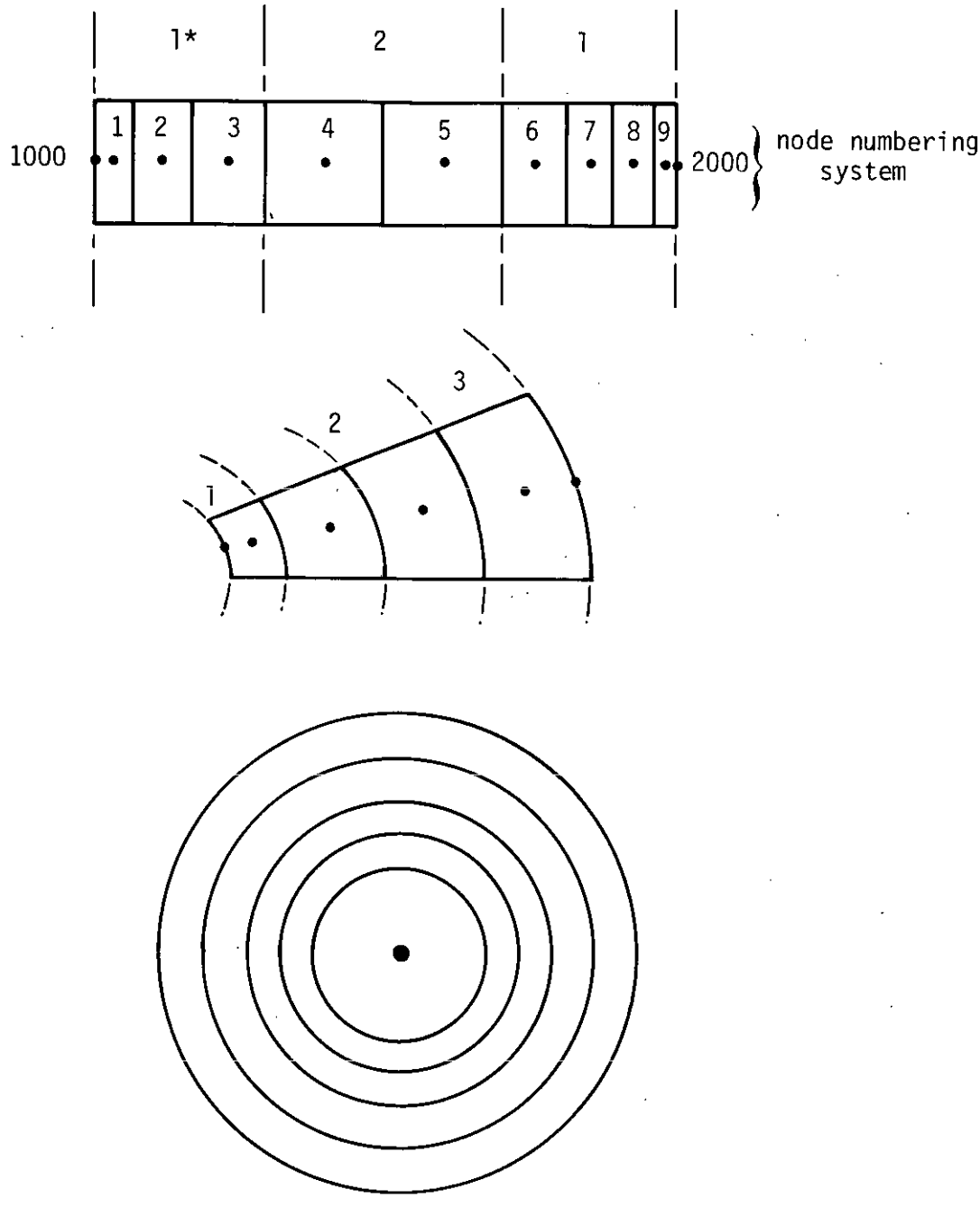

* Numbers signify material types.

Figure 18. Configurations that can be Analyzed by TCY1

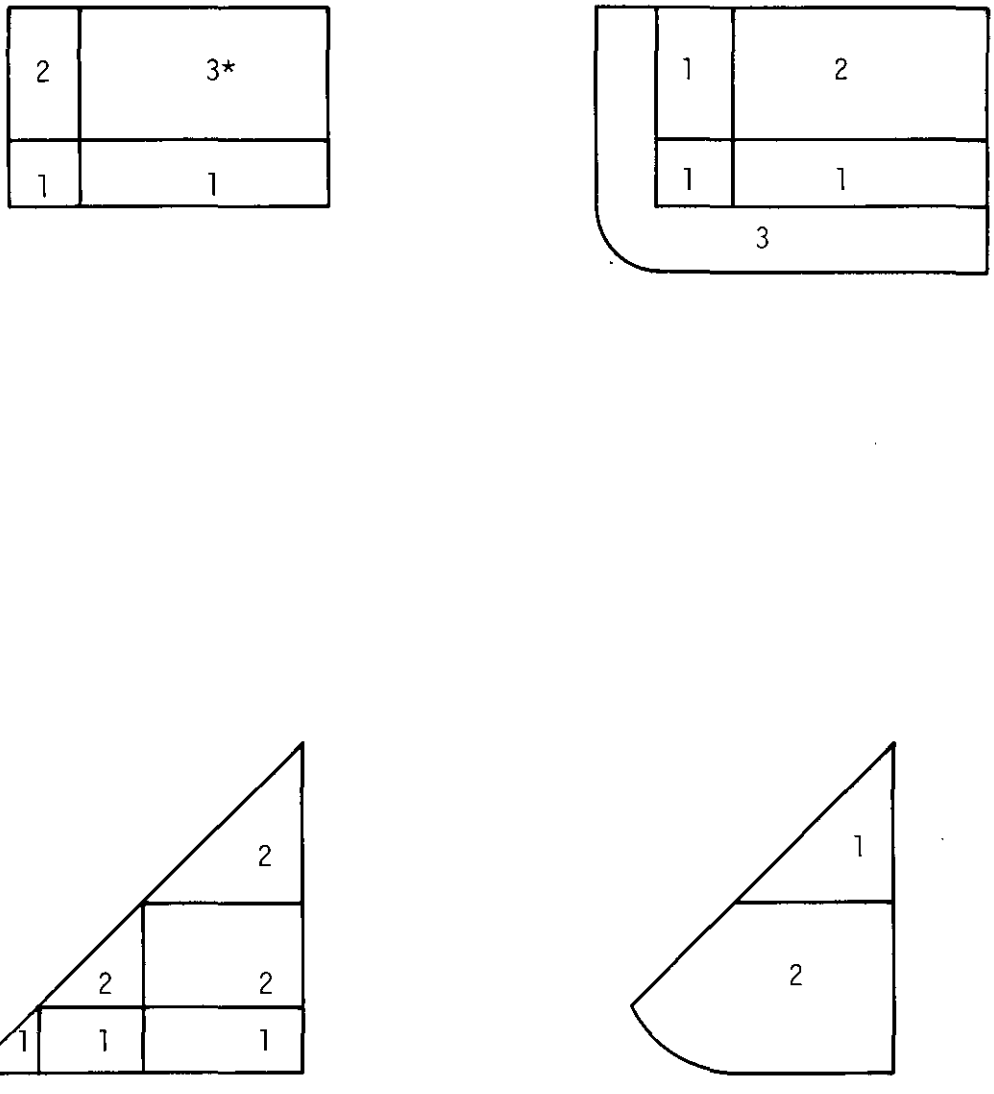

* Numbers signify material types

Figure 19. Configurations that can be Analyzed by TODXY

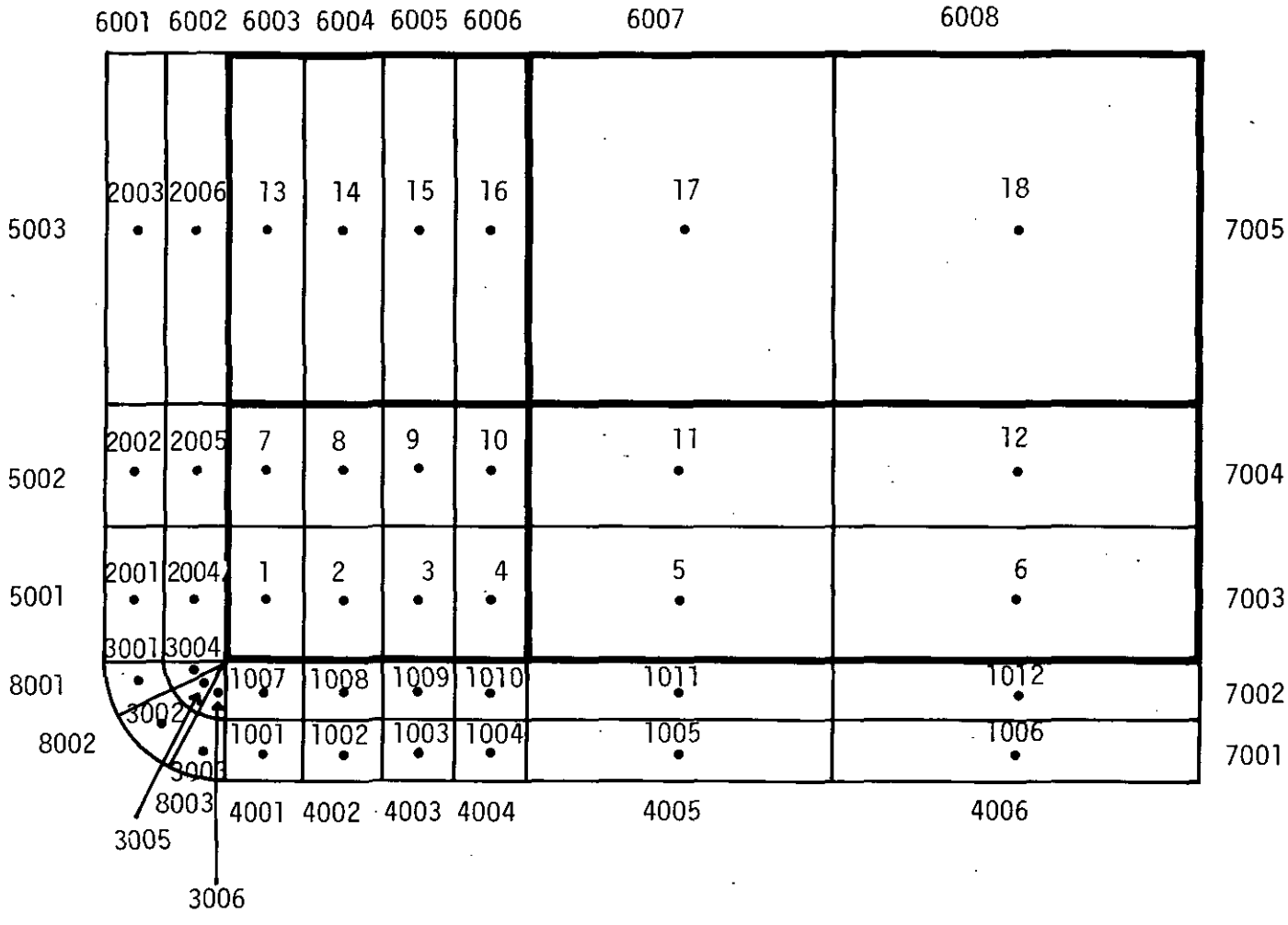

Figure 20. The Basic Node Numbering Scheme Employed by TODXY.

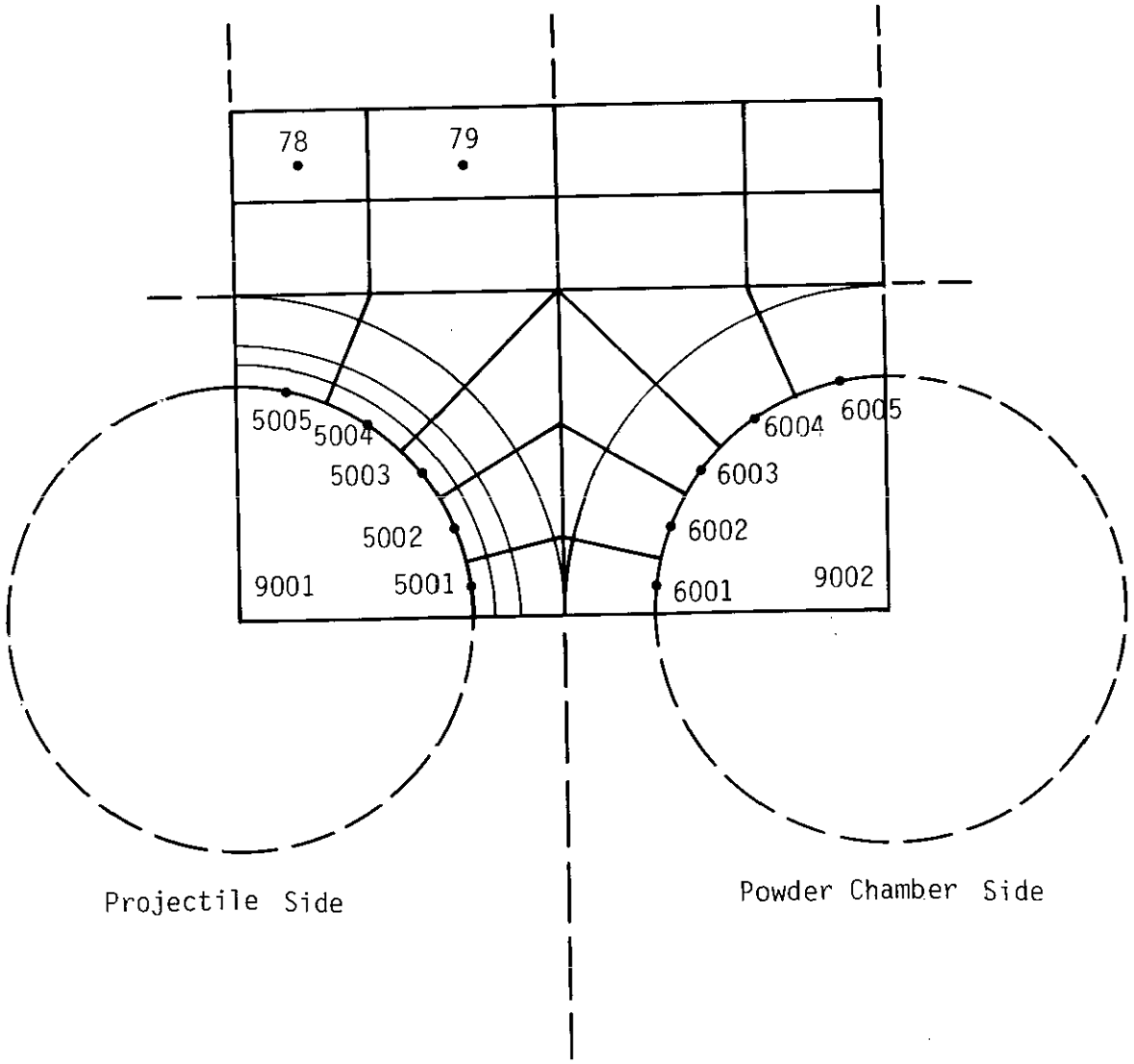

Figure 21. The Geometry and Node Number Scheme of THREED

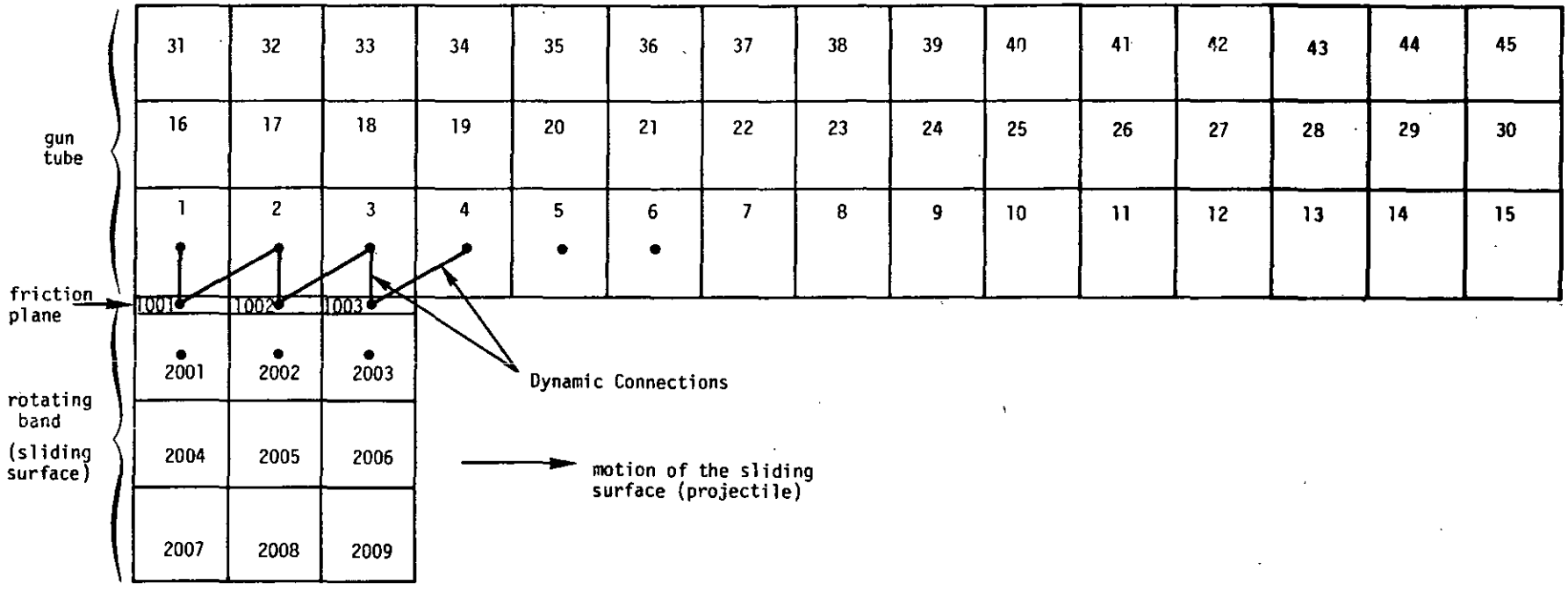

Figure 22. The Basic TRUMP Model of the Sliding Surface Problem

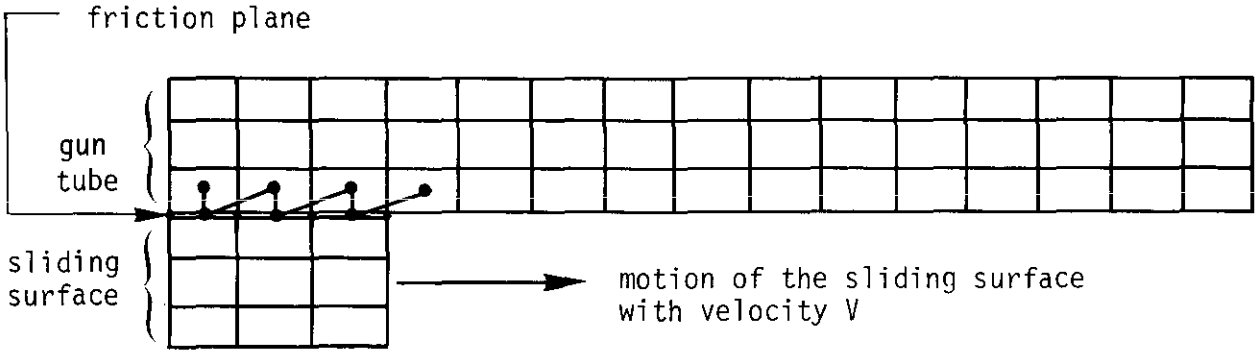

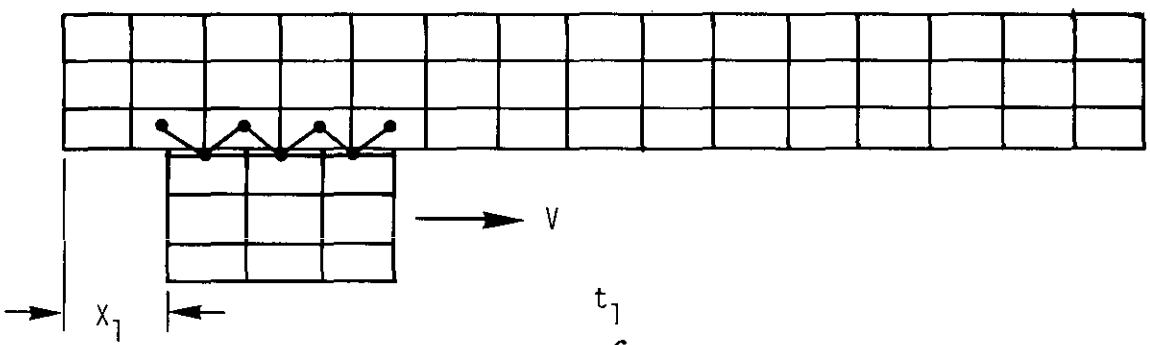

$$X_1 = \int_0^{t_1} V dt$$

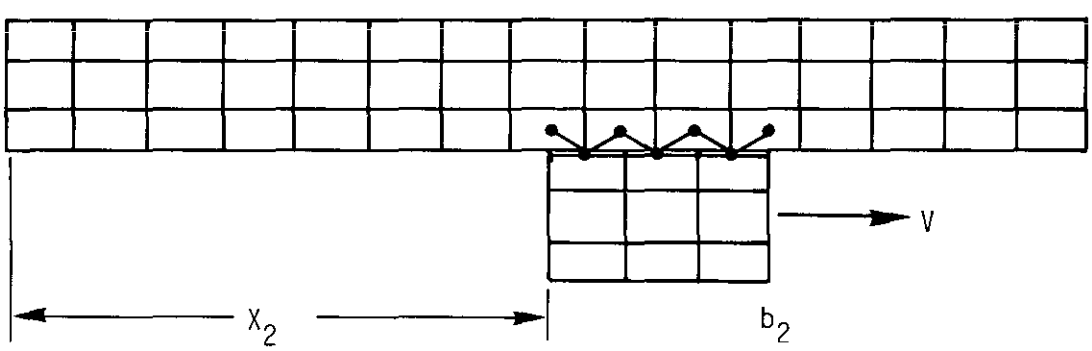

$$X_2 = \int_0^{b_2} V dt$$

Figure 23. TRUMP Simulation of the Sliding Surface Problem

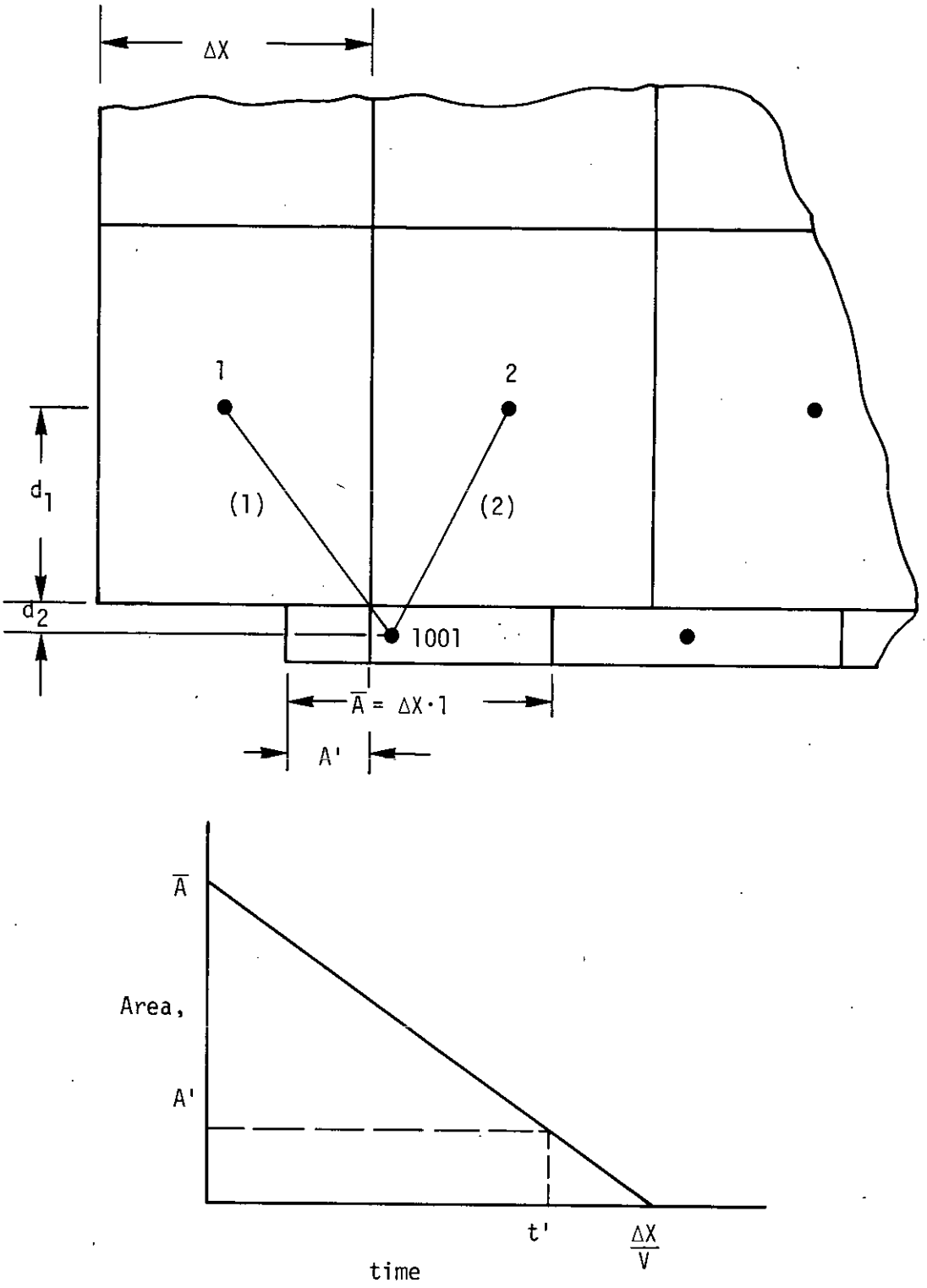

Figure 24. Heat Transfer Area-Time Relationship for Constant Sliding Surface Velocities

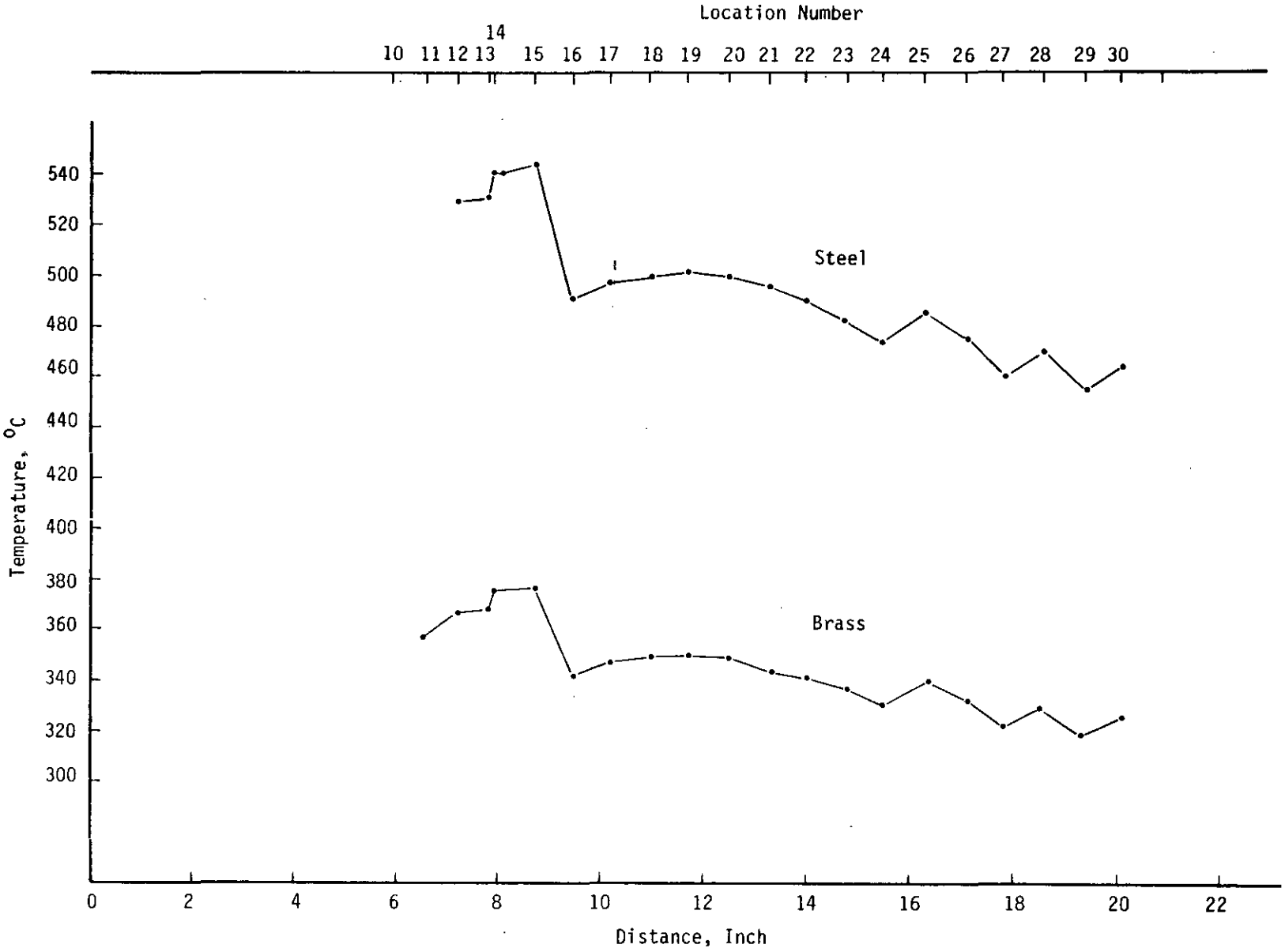

Figure 25. Peak Surface Temperatures as a Function of Distance Along the Gun Tube

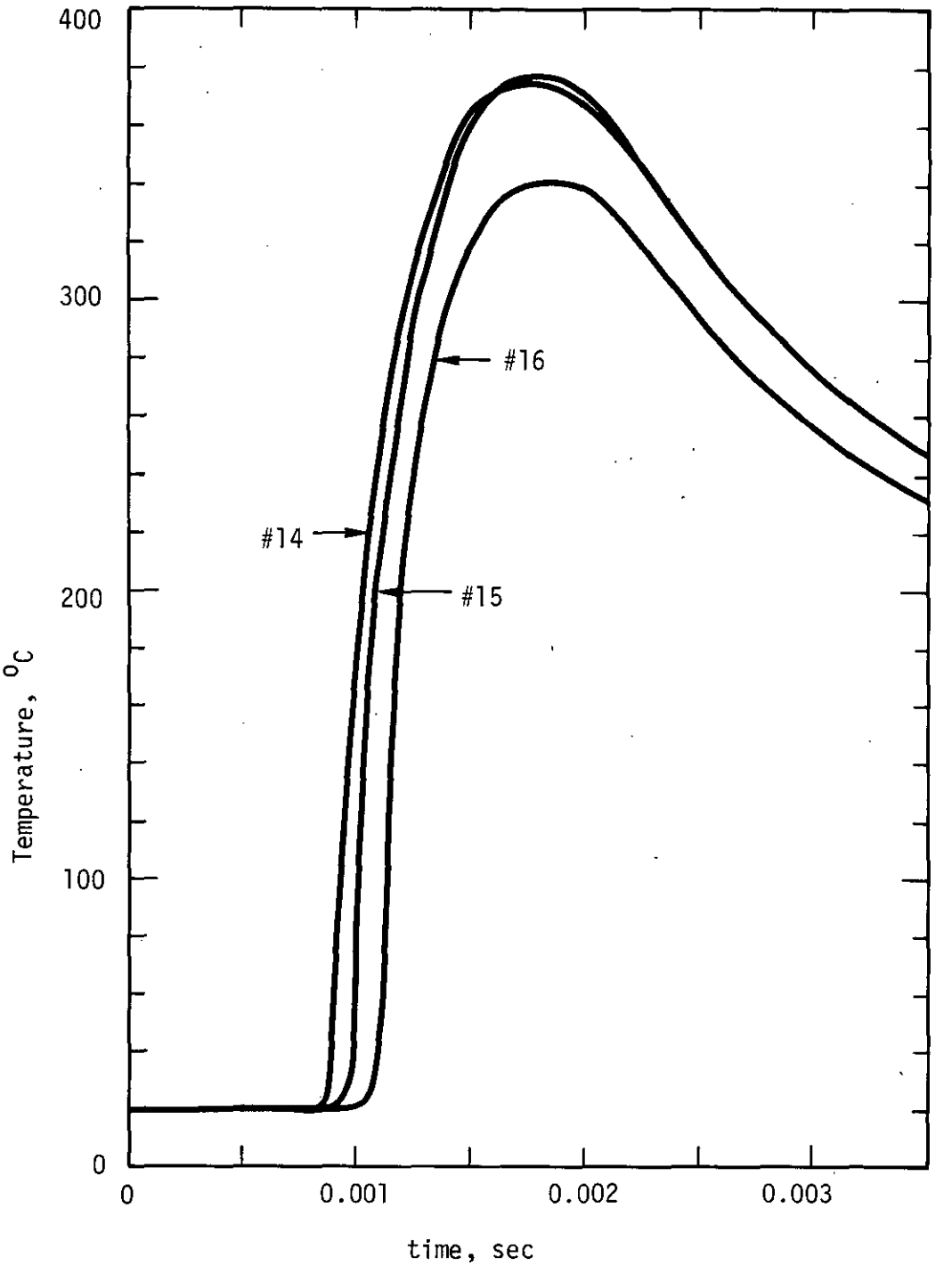

Figure 26. Surface Temperature Histories at Locations 14, 15 and 16

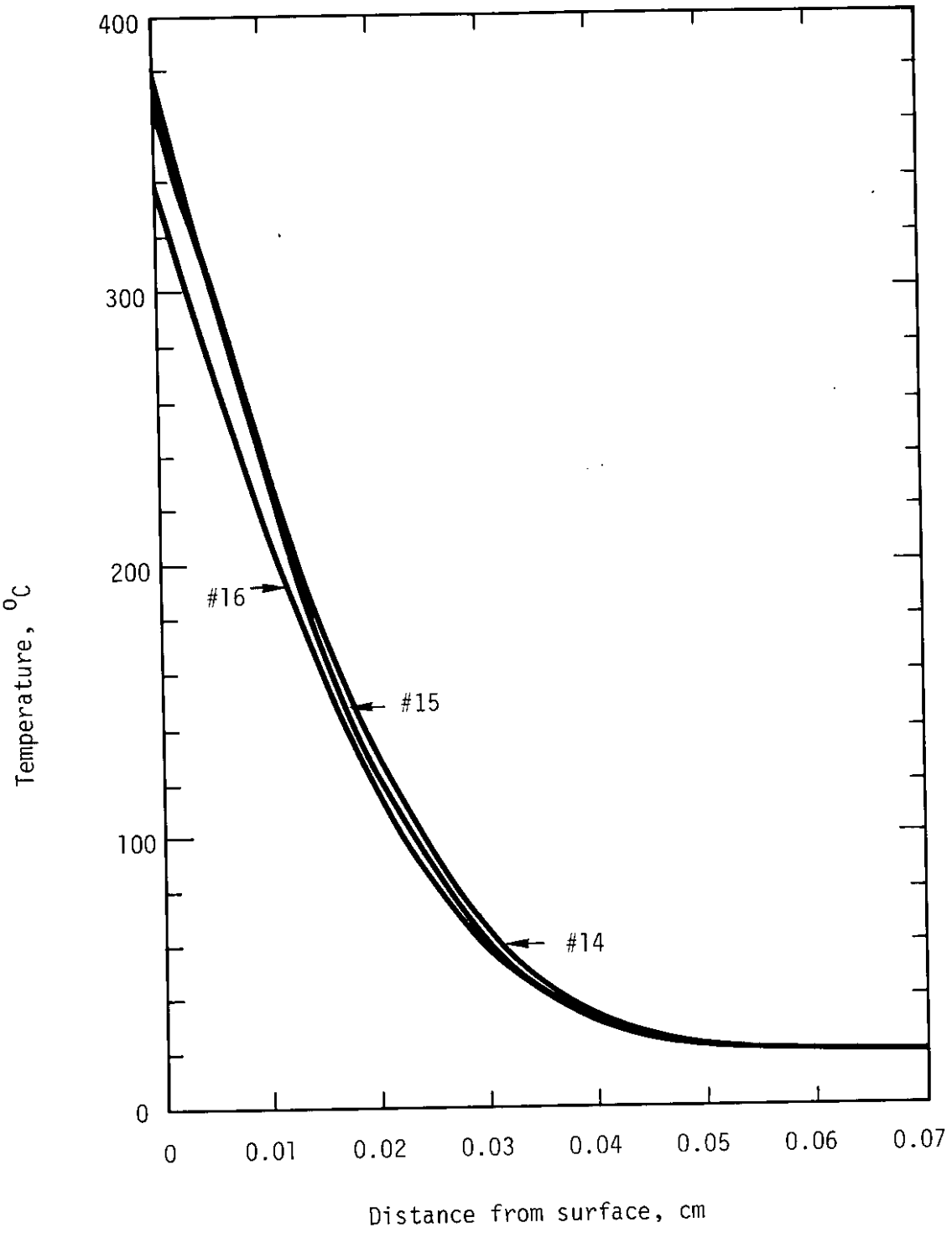

Figure 27. Temperatures Profiles at Locations 14, 15 and 16 at the Time When the Peak Surface Temperature is Experienced

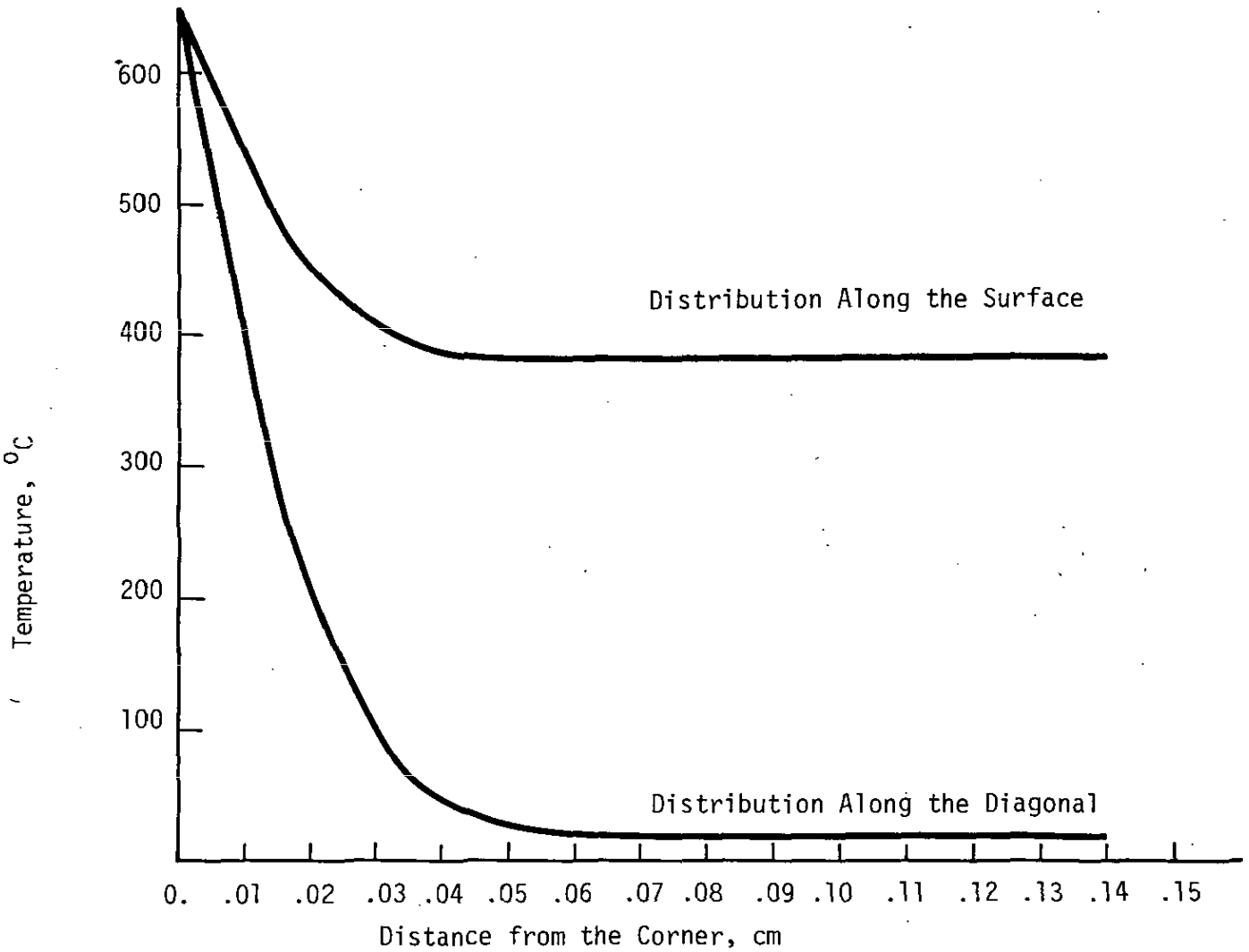

Figure 28. Spatial Temperature Distributions for the Interior Corner Region

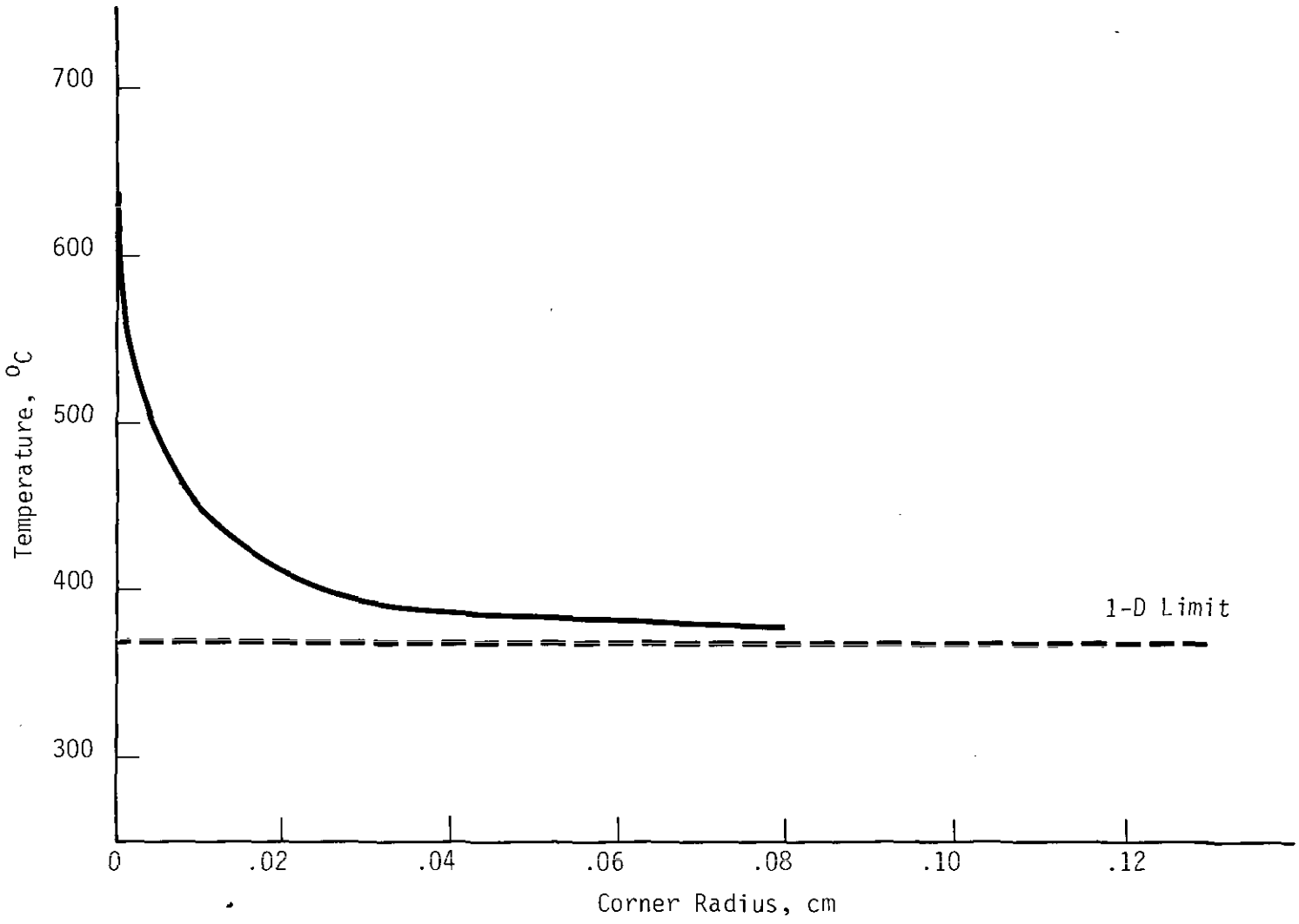

Figure 29. The Effect of Corner Radius on the Peak Surface Temperature

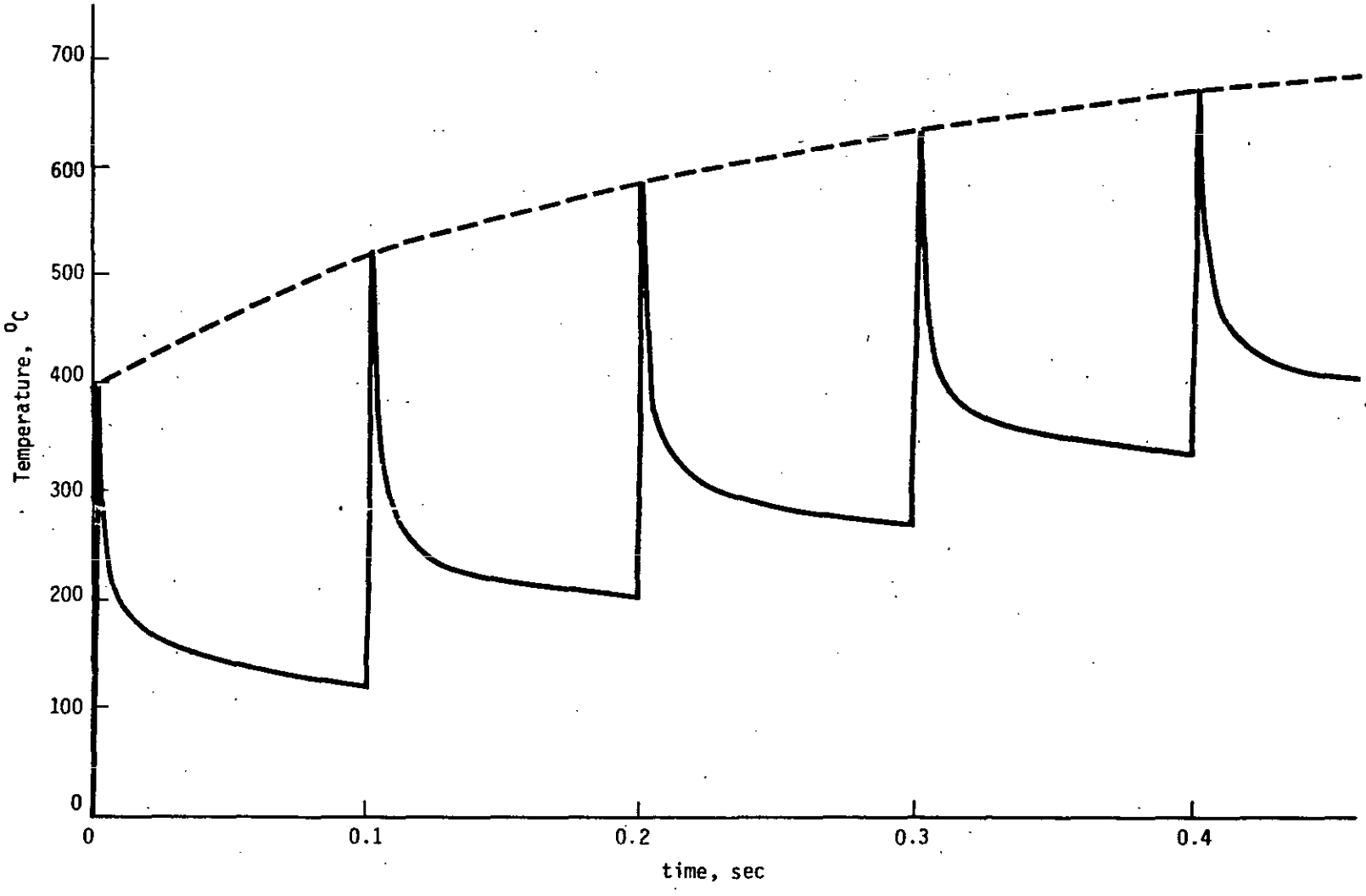

Figure 30. Surface Temperature History at Location 15 for 1-D Multiple Firings

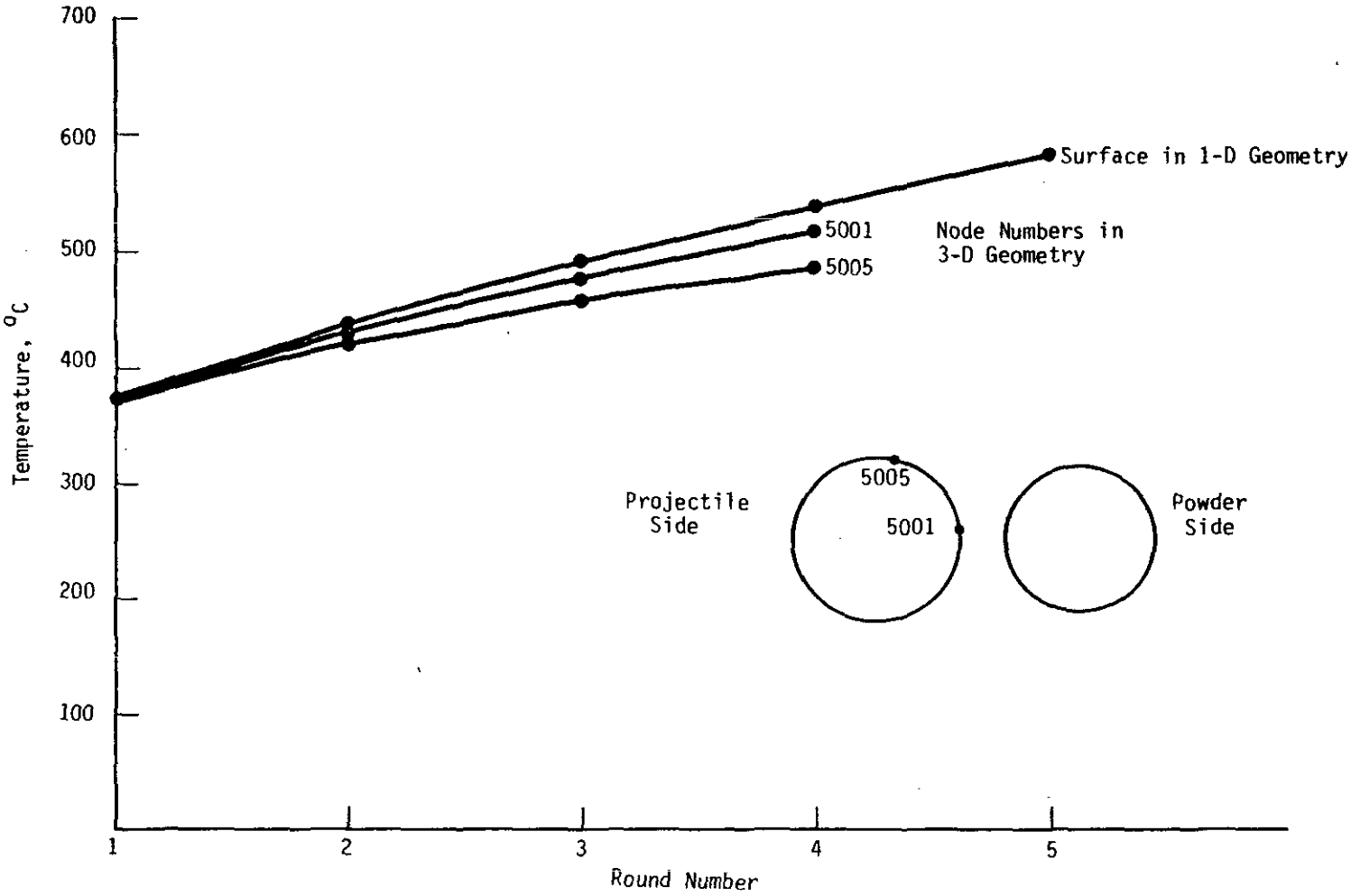

Figure 31. Surface Temperature Histories for 3-D Multiple Firings

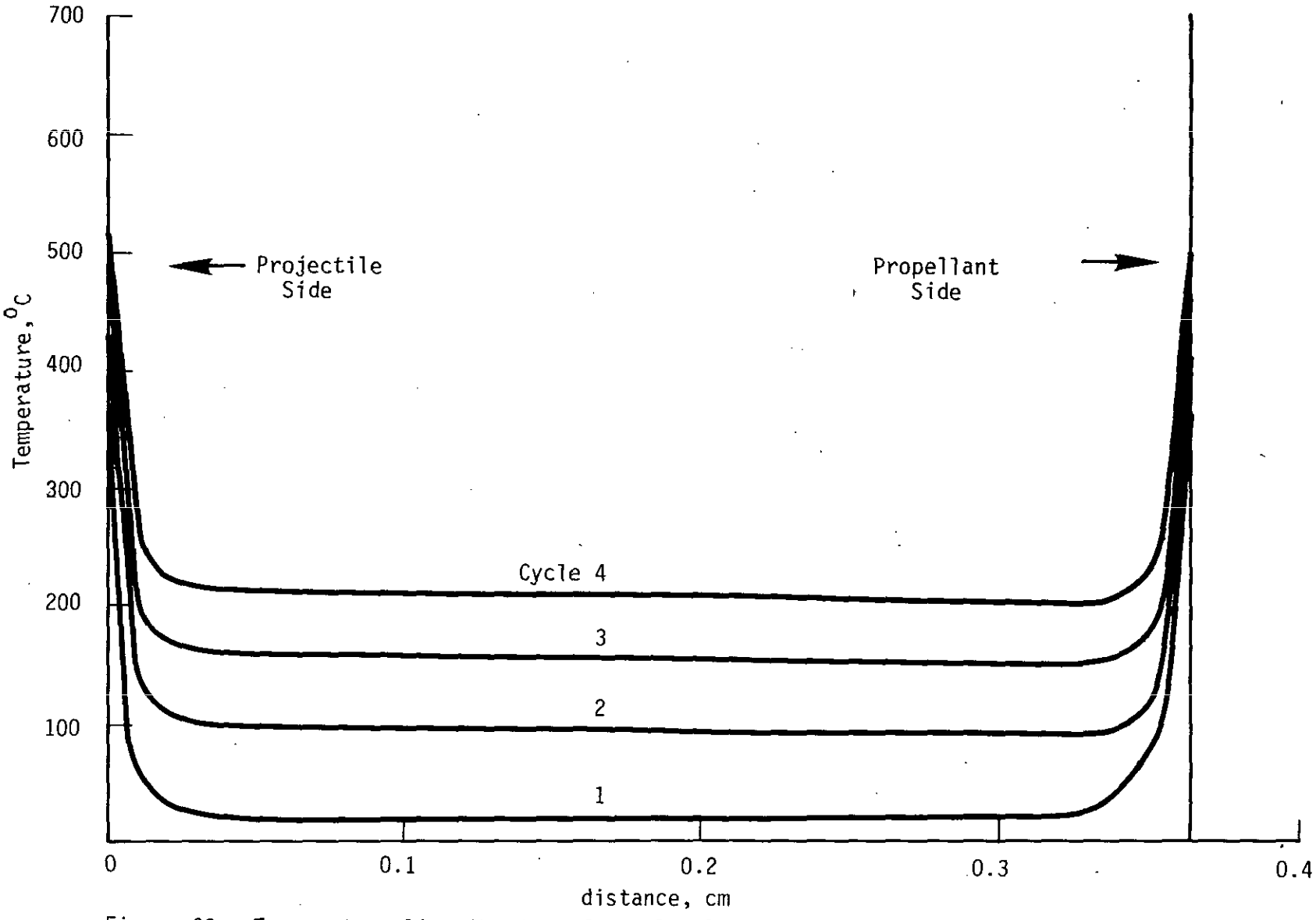

Figure 32. Temperature Distributions for 3-D Multiple Firings

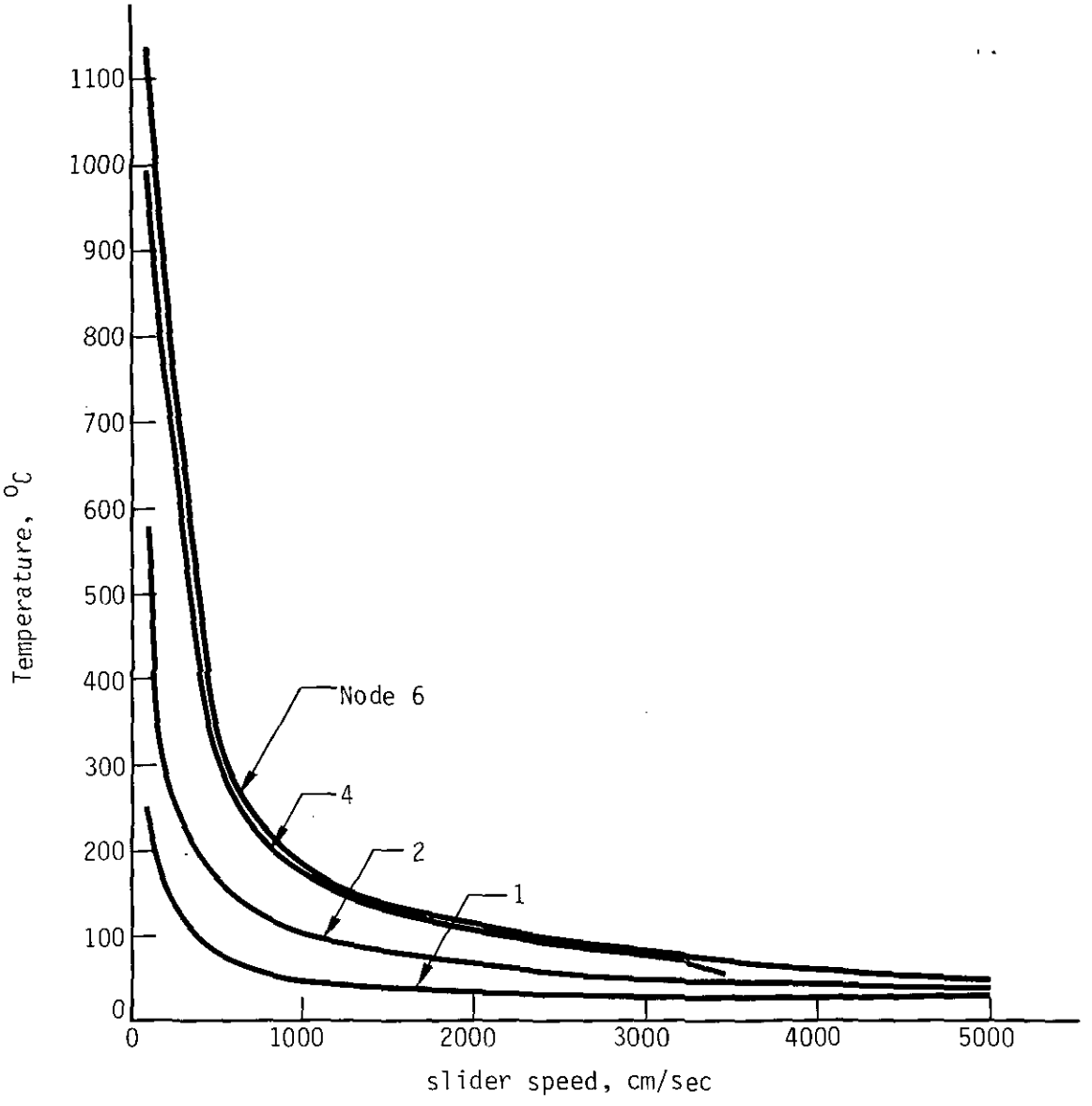

Figure 33. Maximum Temperatures in the Stationary Region as a Function of the Sliding Surface Speed

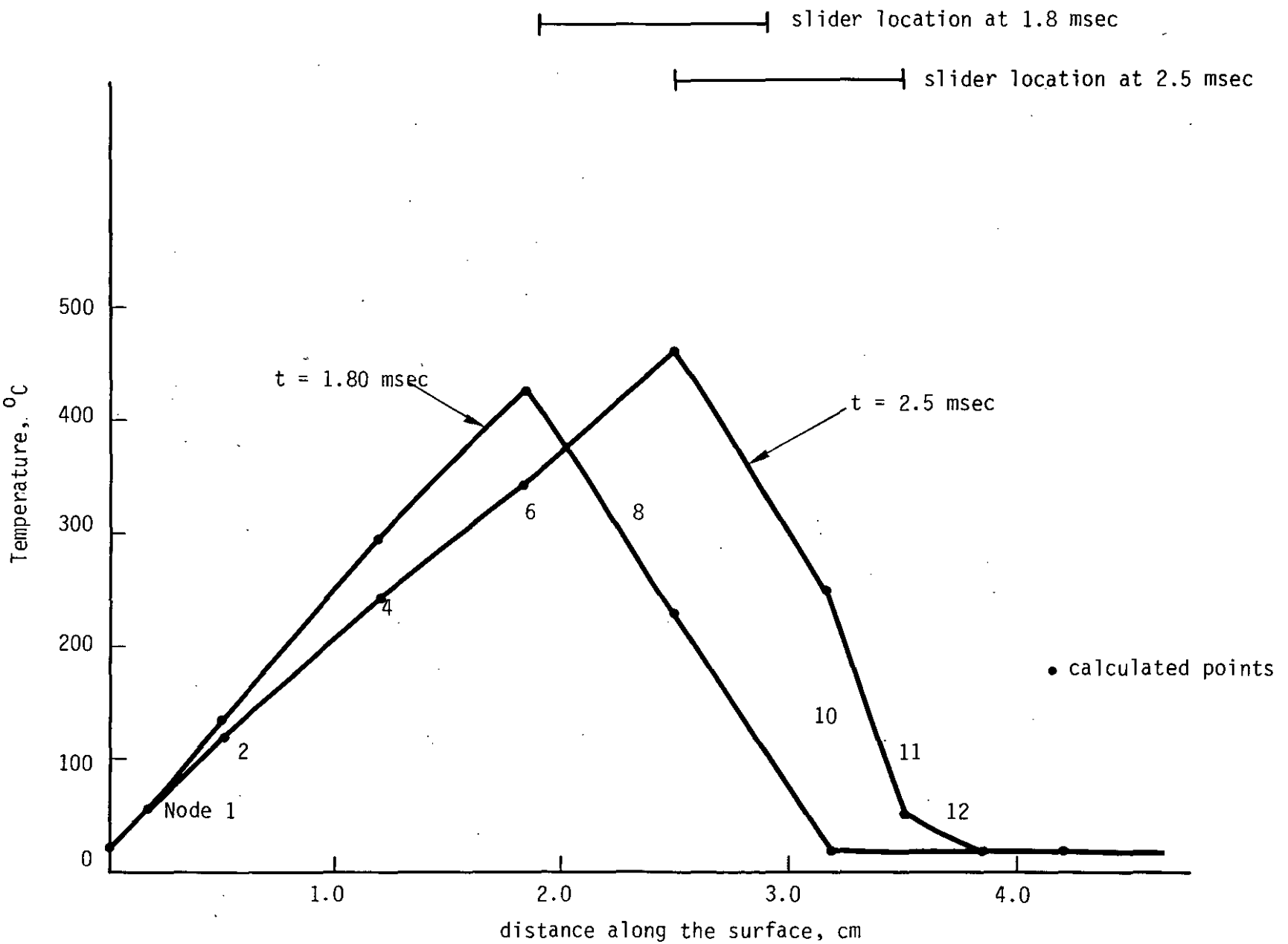

Figure 34. Temperature Distributions in the Stationary Region at Different Times

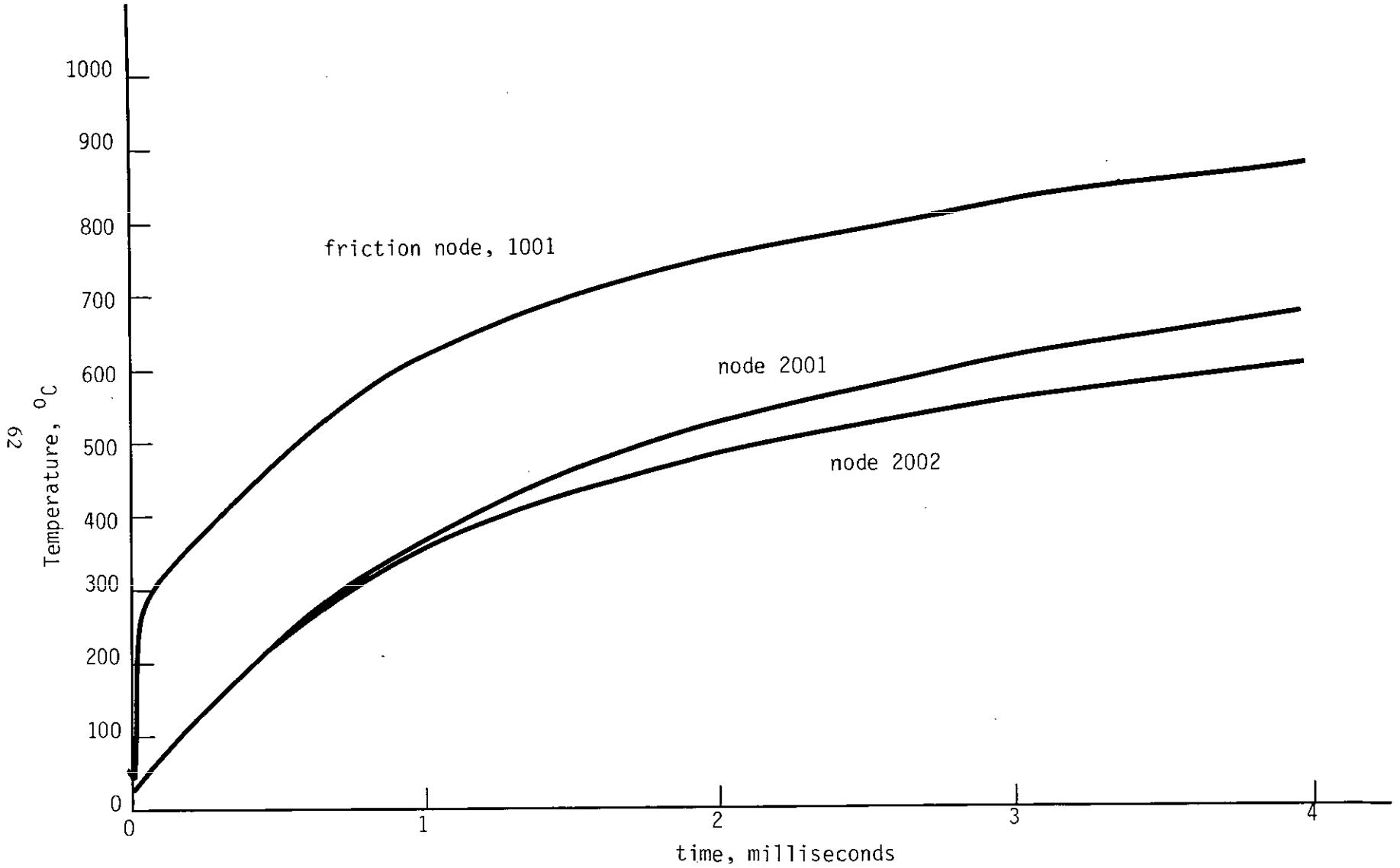

Figure 35. Sliding Surface Temperatures as a Function of Time

DISTRIBUTION LIST

No. of Copies	Organization
12	Commander Defense Documentation Center ATTN: DDC-DDA Cameron Station Alexandria, VA 22314
1	Commander US Army Materiel Development and Readiness Command ATTN: DRCDMD-ST, N. Klein 5001 Eisenhower Avenue Alexandria, VA 22333
1	Commander US Army Aviation Research and Development Command ATTN: DRSAV-E P. O. Box 209 St. Louis, MO 63166
1	Director US Army Air Mobility Research and Development Laboratory Ames Research Center Moffett Field, CA 94035
1	Commander US Army Electronics Research and Development Command Technical Support Activity ATTN: DELSD-L Fort Monmouth, NJ 07703
1	Commander US Army Communications Rsch and Development Command ATTN: DRDCO-PPA-SA Fort Monmouth, NJ 07703
2	Commander US Army Missile Research and Development Command ATTN: DRDMI-R DRDMI-YDL Redstone Arsenal, AL 35809
1	Commander US Army Tank Automotive Research & Development Cmd ATTN: DRDTA-UL Warren, MI 48090
2	Commander US Army Mobility Equipment Research & Development Cmd ATTN: Tech Docu Cen, Bldg. 315 DRSME-RZT Fort Belvoir, VA 22060
3	Commander US Army Armament Research and Development Command ATTN: DRDAR-TSS (2 cys) DRDAR-SCF, S. Goodman Dover, NJ 07801
1	Commander US Army Armament Materiel Readiness Command ATTN: DRSAR-LEP-L, Tech Lib Rock Island, IL 61299
1	Director US Army TRADOC Systems Analysis Activity ATTN: ATAA-SL White Sands Missile Range NM 88002
1	Commander US Army Research Office ATTN: CRD-AA-IP P. O. Box 12211 Research Triangle Park NC 27709
1	Director Lawrence Livermore Laboratory ATTN: Tech Info Div P. O. Box 808 Livermore, CA 94550

DISTRIBUTION LIST

No. of Copies	Organization
1	Director Los Alamos Scientific Lab ATTN: Report Lib P. O. Box 1663 Los Alamos, NM 87544
1	Mathematical Applications Group, Inc. ATTN: E. Troubetzkoy 3 Westchester Plaza Elmsford, NY 10523
1	Science Applications, Inc. ATTN: P. L. Versteegen 8400 Westpark Drive McLean, VA 22101

Aberdeen Proving Ground

Dir, USAMSAA
ATTN: Dr. J. Sperrazza
DRXSY-MP, H. Cohen
Cdr, USATECOM
ATTN: DRSTE-SG-H
Dir, Wpns Sys Concepts Team
Bldg. E3516, EA
ATTN: DRDAR-ACW